


Spring 2015

The pathological role of acrolein in experimental autoimmune encephalomyelitis and multiple sclerosis

Melissa A. Tully
Purdue University

Follow this and additional works at: https://docs.lib.purdue.edu/open_access_dissertations

 Part of the [Biomedical Engineering and Bioengineering Commons](#), [Medicine and Health Sciences Commons](#), [Neuroscience and Neurobiology Commons](#), and the [Nutritional Epidemiology Commons](#)

Recommended Citation

Tully, Melissa A., "The pathological role of acrolein in experimental autoimmune encephalomyelitis and multiple sclerosis" (2015). *Open Access Dissertations*. 573.
https://docs.lib.purdue.edu/open_access_dissertations/573

This document has been made available through Purdue e-Pubs, a service of the Purdue University Libraries. Please contact epubs@purdue.edu for additional information.

PURDUE UNIVERSITY
GRADUATE SCHOOL
Thesis/Dissertation Acceptance

This is to certify that the thesis/dissertation prepared

By Melissa A. Tully

Entitled
THE PATHOLOGICAL ROLE OF ACROLEIN IN EXPERIMENTAL AUTOIMMUNE
ENCEPHALOMYELITIS AND MULTIPLE SCLEROSIS

For the degree of Doctor of Philosophy

Is approved by the final examining committee:

Riyi Shi

Kevin Hannon

Eric Nauman

Kevin Otto

To the best of my knowledge and as understood by the student in the Thesis/Dissertation Agreement, Publication Delay, and Certification/Disclaimer (Graduate School Form 32), this thesis/dissertation adheres to the provisions of Purdue University's "Policy on Integrity in Research" and the use of copyrighted material.

Riyi Shi

Approved by Major Professor(s): _____

Approved by: George Wodicka

04/20/2015

Head of the Department Graduate Program

Date

THE PATHOLOGICAL ROLE OF ACROLEIN IN EXPERIMENTAL
AUTOIMMUNE ENCEPHALOMYELITIS AND MULTIPLE SCLEROSIS

A Dissertation

Submitted to the Faculty

of

Purdue University

by

Melissa A. Tully

In Partial Fulfillment of the
Requirements for the Degree

of

Doctor of Philosophy

May 2015

Purdue University

West Lafayette, Indiana

To my family, for their endless love and support

ACKNOWLEDGEMENTS

I was extremely fortunate throughout the duration of this challenging journey to have the unwavering support of my family, friends, colleagues and faculty advisors. My deepest gratitude goes to everyone who worked hard to make my graduate career at Purdue a success.

First and foremost, I would like to thank my faculty advisor Dr. Riyi Shi for his mentorship and encouragement over the past four years. His infectious attitude and genuine passion for science fueled my drive to continue on my quest for discovery and made pursuing a Ph.D. an enjoyable experience. It has been my sincere pleasure to have had the opportunity to learn and receive training in his laboratory. Next, I would like to thank the members of my graduate committee, Dr. Kevin Hannon, Dr. Eric Nauman and Dr. Kevin Otto, for their praises and criticisms, equally, as they have both encouraged and challenged me to become a better scientist. Thank you to my faculty collaborators Dr. Bruce Cooper and Dr. David Mattson for their expertise. Also, thank you to the directors of the Indiana University School of Medicine MSTP program, Dr. Maureen Harrington and Dr. Raghu Mirmira, for their continuous encouragement. Special thanks to Sandy May and Jan Receveur for your patience and helping me with administrative issues because if you know me at all, you know I have had many.

My time here at Purdue has been greatly enhanced by having the opportunity to work with some very intelligent and wonderful people. I would like to thank Dr. Gary Leung and Dr. Wenjing Sun for initiating the EAE study and patiently teaching me all of the lab skills that I needed to independently conduct the study upon their graduation; Dr. Sean Connell- for helping me whenever I needed to engineer and construct something on a budget; Dr. Jonghyuck Park, Dr. Désirée Schenck, Dr. Lingxing Zheng, Glen Acosta, Nick Race and Ran Tian- for their collaborative efforts and willingness to help with troubleshooting when I experienced difficulties.

Finally and most importantly, I would like to thank my family. I am extremely fortunate to have a strong support system. Thank you to my parents for always being there, no matter what, to my sister for always telling me the truth and keeping me grounded and to my brother for making me laugh when things got a little too serious. Words cannot even begin to express the how grateful I am for you guys.

TABLE OF CONTENTS

	Page
LIST OF TABLES	viii
LIST OF FIGURES	ix
LIST OF ABBREVIATIONS	xi
ABSTRACT	xiii
CHAPTER 1. INTRODUCTION	1
1.1 Clinical Features of Multiple Sclerosis	1
1.2 Multiple Sclerosis Subtypes and Diagnostic Criteria	3
1.3 Pathogenesis of Multiple Sclerosis	5
1.4 Oxidative Stress-Induced Damage to Axolemma and Myelin	7
1.5 The Neurotoxic Nature of Acrolein	7
1.5.1 Acrolein-Mediated Demyelination	9
1.5.2 Acrolein-Induced Axonal Injury in Multiple Sclerosis	10
1.5.3 Impairment of Mitochondrial Processes by Acrolein	11
CHAPTER 2. NEUROPROTECTIVE ROLE OF ACROLEIN SCAVENGERS IN EAE	13
2.1 Introduction	13
2.2 Acrolein-Lysine Adducts Increased in EAE Spinal Cord Tissue ..	15
2.3 Hydralazine Attenuated Behavioral Deficit and Myelin Damage in EAE Mice	16
2.4 Application of Hydralazine at Time of Symptom Emergence	20
2.5 Summary and Significance	21
CHAPTER 3. ALLEVIATION OF BEHAVIORAL DEFICITS IN EAE USING ALTERNATIVE ACROLEIN SCAVENGERS	22
3.1 Introduction	22
3.2 Materials and methods	22
3.2.1 EAE mice	22
3.2.2 Behavioral Assessment	23
3.2.3 In vivo Phenzelzine treatment	23
3.2.4 In vivo EGCG treatment	23
3.2.5 Spinal Cord Tissue Preparation	24
3.3 Phenzelzine	24
3.4 Epigallocatechin gallate	27
3.5 Discussion	29
CHAPTER 4. APPLICATION OF PEG AS A MEMBRANE REPAIR AGENT	30

	Page
4.1	Introduction..... 30
4.2	Materials and methods 32
4.2.1	EAE Mice..... 32
4.2.2	Horseradish Peroxidase Exclusion Test..... 32
4.2.3	PEG treatment and Preparation 33
4.3	Results..... 33
4.3.1	Axonal Membrane Damage and Its Alleviation by PEG 33
4.3.2	PEG Treatment Significantly Reduced Symptom Severity and Delayed Disease Onset in EAE Mice 35
4.4	Discussion 37
CHAPTER 5.	ESTABLISHMENT OF ACROLEIN DETECTION METHODS.. 40
5.1	Introduction..... 40
5.1.1	GC and LC/MS-based techniques 40
5.1.2	Antibody Detection of Acrolein-Protein Adducts 41
5.1.3	3-HPMA Detection Using LC/MS/MS 42
5.1.4	Translational Nature of Acrolein Research 43
5.2	Materials and methods 43
5.2.1	Animal Preparation..... 43
5.2.2	EAE Model Induction and Behavioral Assessment..... 44
5.2.3	Dot Immunoblotting 44
5.2.4	Animal Urine Collection 45
5.2.5	Subject Enrollment 45
5.2.6	Clinical Urine Collection..... 45
5.2.7	Clinical Serum Collection..... 46
5.2.8	3-HPMA Quantification Using LC/MS/MS..... 46
5.3	Results..... 48
5.3.1	CNS and Systemic Elevation of Acrolein in EAE Mice 48
5.3.2	Multiple Sclerosis Patients Exhibited Increased 3-HPMA in Urine and Serum 51
5.4	Concluding Summary 56
CHAPTER 6.	RESPIRATORY EXPOSURE TO ACROLEIN..... 59
6.1	Introduction..... 59
6.1.1	Cigarette Smoking in Humans 60
6.1.2	Acrolein Inhalation in Mice..... 61
6.2	Materials and methods 62
6.2.1	Respiratory Exposure to Exogenous Acrolein 62
6.2.2	GC/MS..... 63
6.2.3	Detection of Acrolein-Lysine Adducts 63
6.2.4	3-HPMA Quantification 63
6.2.5	Subject Recruitment 63
6.2.6	Clinical Urine Collection..... 64
6.3	Results..... 64
6.3.1	Urine 3-HPMA Increased Following Acrolein Inhalation 64

	Page
6.3.2 Respiratory Acrolein Exposure Increases Acrolein-Lysine Adducts in Mouse Spinal Cord Tissue.....	64
6.3.3 Systemic 3-HPMA Elevation in MS Patients Who are Self- Reported Cigarette Smokers	67
6.4 Discussion	69
CHAPTER 7. ACROLEIN ELEVATION IN BOTH RR MS PATIENTS AND RR EAE AND SYMPTOM ALLEVIATION IN RR EAE BY HYDRALAZINE	72
7.1 Introduction.....	72
7.2 Materials and methods	72
7.2.1 Subject Recruitment.....	72
7.2.2 Clinical Urine collection	72
7.2.3 Clinical Serum Collection.....	73
7.2.4 RR EAE Induction and Behavioral Assessment	73
7.2.5 Hydralazine Preparation and Application.....	73
7.2.6 Animal Urine Collection	74
7.2.7 3-HPMA Analysis	74
7.2.8 Dot Immunoblotting	74
7.3 Preliminary Results	74
7.3.1 Clinical 3-HPMA Elevations in Urine and Serum of RR MS Patients	74
7.3.2 Daily Hydralazine Application Ameliorated Motor Deficit in RR EAE	74
7.4 Discussion of Preliminary Findings.....	77
CHAPTER 8. FURUTE DIRECTIONS.....	79
8.1 Examine the Effects of Exogenous Acrolein Exposure on Development of the EAE Model.....	80
8.2 Employment of Minimally Invasive Neuroimaging Techniques with 3-HPMA Quantification to Determine How Endogenous Acrolein Concentration Corresponds with CNS Structural Damage	80
REFERENCES	81
VITA	91

LIST OF TABLES

Table	Page
Table 1.1 Clinical Signs and Symptoms of Multiple Sclerosis.....	2
Table 1.2 Defintions of McDonald Criteria Terms	4
Table 1.3 McDonald Criteria for diagnosis of multiple sclerosis.....	5

LIST OF FIGURES

Figure	Page
Figure 2.1 Induction of EAE Model	14
Figure 2.2 Acrolein Scavenging by Hydralazine	15
Figure 2.3 Dot Immunoblotting Quantification of Acrolein-Lysine Adducts in Spinal Cord.....	16
Figure 2.4 Hydralazine Therapy Ameliorated Motor Deficits.	18
Figure 2.5 Attenuation of Acrolein-Lysine Adducts by Hydralazine Treatment ...	19
Figure 2.6 Hydralazine Application at Symptom Onset.	20
Figure 3.1 Acrolein Scavenging by Phenelzine	26
Figure 3.2 Behavioral Assessment of Sham-Treated and Phenelzine-Treated EAE Mice.....	27
Figure 3.3 Phenelzine Attenuated Behavioral Deficit in EAE.....	27
Figure 3.4 Phenelzine delayed Symptomatic Onset in EAE Mice.....	28
Figure 3.5 Behavioral assessment of sham-treated and EGCG-treated EAE mice	29
Figure 4.1. Axonal Membrane Damage in EAE and its Alleviation by PEG.....	35
Figure 4.2 Evaluation of PEG as a Therapy for EAE Axonal Damage.....	37
Figure 4.3. PEG Delayed Symptom Onset in EAE Mice.....	38
Figure 5.1 Behavioral Deficits Following MOG EAE Induction.....	50
Figure 5.2. Determination of Acrolein Concentration Through Urine 3-HPMA Measurement in EAE Mice.	51
Figure 5.3. Elevations of CNS Acrolein Concentrations in EAE Mice	52
Figure 5.4. Determination of Acrolein Concentration Through Urine 3-HPMA Measurement in MS Patients and Healthy Individuals.....	54
Figure 5.5. Determination of Acrolein Concentration Through Serum 3-HPMA Measurements in MS Patients and Healthy Individuals.....	55
Figure 5.6. Correlation of 3-HPMA Levels in Urine and Serum in MS Patients. .	56
Figure 6.1. Preclinical Assessment of the Effects of Respiratory Acrolein Exposure in Mice.	66

Figure	Page
Figure 6.2. Smoking in MS Patients is Associated with Higher Urine 3-HPMA...	68
Figure 6.3. Smoking Cigarettes is Associated with Higher EDSS Scores in Multiple Sclerosis Patients.	68
Figure 7.1. Quantification of 3-HPMA in the Urine and Serum of RR MS Patients.	76
Figure 7.2. Hydralazine Application in RR EAE Augments Motor Function	77

LIST OF ABBREVIATIONS

3-HPMA	3-Hydroxypropyl Mercapturic Acid
ATP	Adenosine Triphosphate
BSA	Bovine Serum Albumin
CDC	Center for Disease Control
CNS	Central Nervous System
EAE	Experimental Autoimmune Encephalomyelitis
EGCG	Epigallocatechin gallate
EI	Electron Impact
FDA	Food and Drug Administration
GC	Gas Chromatography
GSH	Glutathione
HRP	Horseradish Peroxidase
LC/MS	Liquid Chromatography/Mass Spectrometry
LPO	Lipid Peroxidation
MAO-I	Monoamine Oxidase Inhibitor
MOG	Myelin Oligodendrocyte Glycoprotein
MS	Multiple Sclerosis
OCT	Optimum Cutting Temperature
PBS	Phosphate Buffer Saline

PEG	Polyethylene Glycol
PLP	Proteolipid Lipoprotein
PP	Primary Progressive
ROS	Reactive Oxygen Species
RR	Relapsing Remitting
SP	Secondary Progressive
VGK	Voltage-Gated Potassium

ABSTRACT

Tully, Melissa A. Ph.D., Purdue University, May 2015. The Pathological Role of Acrolein in Experimental Autoimmune Encephalomyelitis and Multiple Sclerosis. Major Professor: Riya Shi.

Multiple sclerosis (MS) is an autoimmune demyelinating neuropathy that affects nearly 2.5 million people worldwide. Despite substantial efforts, few treatments are currently available largely due to limited knowledge of pathogenic mechanisms underlying the disease. The immune-inflammatory nature of the pathology has prompted investigation of the role of oxidative stress in disease development and progression; however targeting reactive oxygen species for neutralization has had marginal success therapeutically, suggesting that an alternate oxidative stress-related target would prove beneficial. Recently, our lab has implicated acrolein, a highly reactive aldehyde that is both a byproduct and catalyst of lipid peroxidation, as a potential therapeutic target and biomarker for MS diagnosis and symptom monitoring. We have shown that acrolein is elevated in clinical MS cases and experimental autoimmune encephalomyelitis (EAE), a murine model of MS. Furthermore, pharmacological sequestering of acrolein afforded a neuroprotective effect by suppressing tissue acrolein level, slowing disease progression, and decreasing symptom severity. Acrolein can also be produced exogenously as a pollutant from combustion engine exhaust, industrial processing, burning of

tobacco and overheated cooking oil vapors. The pathogenic role of endogenous acrolein in MS raises the possibility that environmental exposure to acrolein could potentially increase MS risk or exacerbate MS symptoms. Using a respiratory exposure model in combination with urinary detection of an acrolein metabolite and immunoblotting assessment of tissue acrolein-lysine adducts, we have ascertained that inhalation of acrolein can cause accumulation of acrolein in mice systemically and locally within the CNS. Additionally clinical acrolein assessment using urine and serum samples revealed that MS patients who self-reported as smokers demonstrated higher systemic acrolein levels and demonstrated greater motor deficit compared to MS patients that did not smoke. These observations indicate that acrolein is likely contributing to the mechanisms underlying symptom development in EAE and MS and may serve as a therapeutic target and biomarker for diagnosis, guiding treatment regimens and monitoring relapses.

CHAPTER 1. INTRODUCTION

1.1 Clinical Features of Multiple Sclerosis

Multiple sclerosis (MS) is an immune-mediated demyelinating disorder of the central nervous system (CNS) that affects 1 of 1,000 people in the United States and approximately 2.5 million globally. Two of three MS patients is female and on average exhibit an onset of symptoms five years earlier than their male counterparts [1, 2]. Along with differing risk associated with gender, MS incidence and prevalence also appear to be related to geography, most commonly presenting in Caucasians living in the cooler climates of the Northern hemisphere. With an average onset of 23.5 years, MS patients have a mean life expectancy of 50 years and often require assistance with daily activities 10 years following diagnosis due to severe disability [2, 3]. Additionally, patients were 3 times more likely to experience premature mortality than the unaffected population by 38 years following symptom onset [4]. With an annual patient cost of care of 47,000 dollars and as a disease that presents relatively early in life, MS poses a substantial financial burden on patients, their families, and society [5]. Furthermore, MS patients are at greater risk of presenting with concomitant autoimmune diseases such as autoimmune thyroid disease, type I diabetes mellitus, and inflammatory bowel disease, perpetuating financial stress associated with increased healthcare cost [6-9].

Due to a global assault of CNS white matter tracts, MS presents clinically as a collection of neurological sequelae that can often be mistaken as unrelated [10]. Table 1.1 outlines patient-reported symptoms and/or those observed upon physical examination for which an MS diagnosis should be considered.

Table 1.1 Clinical signs and symptoms of multiple sclerosis; adapted from [11]

Symptoms	Description	% Affected	% Presenting
Sensory Disturbances	Intense itching, numbness, tingling, pins and needles, tightness, coldness, impairment of joint position sense, swelling	100	30.7
Pain	Trigeminal neuralgia, Lhermitte's sign, dysesthesia, back/visceral pain, tonic spasms	40.3	0.5
Balance/ Gait Disturbances, Ataxia	Observed deviation in walking pattern, limb discoordination	30-50	8.9
Vertigo	Severe dizziness, specifically a movement hallucination	45	1.7
Visual Deficits	Complete/parital loss, optic neuritis, internuclear ophthalmoplegia, diplopia	15-75	15.9

Bowel/Bladder Dysfunction	Urgency, incontinence, constipation	--	1
Sexual Dysfunction	Complete; Impaired	50;20	--

1.2 Multiple Sclerosis Subtypes and Diagnostic Criteria

MS presentation can differ in average age of onset, time course, and rate of symptom progression, which resulted in the establishment of two main subtypes: relapsing remitting (RR) and primary progressive (PP) [12]. RR MS accounts for approximately 85% of cases, tends to present in younger patients between 25 and 33 years old and is characterized by transient CNS attacks with either partial or complete symptomatic resolution, occurring one to two times per year. However, RR MS patients generally transition into a phase deemed secondary progressive (SP) at 40-44 years old in which they exhibit attacks without recovery. Absence of recovery following an attack and the resulting slow, steady deterioration of the patient is believed to correspond to permanent neurological impairment attributed to axonal degeneration and loss of neuroplasticity [13]. PP MS is responsible for the other 15% of cases and presents in older patients averaging from 35 to 39 years old [14]. PP MS shares many characteristics with SP MS, except that it is not preceded by RR MS; PP MS patients, even in early stages of the disease, do not experience physical recovery following an attack.

The diagnostic criteria for MS are explicitly described in the McDonald Criteria which was first created in 2001 and outlines combinations of physical examination findings and laboratory testing to afford sufficient evidence to

definitively diagnose MS [15]. Since its inception, the Criteria have been revised twice, once in 2005 and again in 2010, to incorporate further knowledge gained pertaining to the disease as well as to account for advances in technology [16-19]. These revisions preserved both sensitivity and specificity of the Criteria as a diagnostic tool and also the classification of symptoms as either disseminated in space or in time (Table 1.2) [20]. Complete demonstration of any of the combinations of parameters outlined in the criteria justifies a definitive MS diagnosis (Table 1.3). The diagnosis of “possible MS” can be made if an MS diagnosis is suspected, but some pieces of the criteria are absent. If the requirements of the criteria are not met, other disorders should be considered.

Table 1.2 Definitions of McDonald Criteria Terms; adapted from [20]

<p>Dissemination in Space (DIS)</p>	<p>MRI shows: ≥ 1 T2 lesion in ≥ 2 of the following areas:</p> <ul style="list-style-type: none"> • Periventricular • Juxtacortical • Infratentorial • Spinal cord
<p>Dissemination in Time (DIT)</p>	<p>A new T2 or Gd-enhancing lesion on follow-up MRI (not dependent on timing of first scan) OR Gd-enhancing lesion(s) and non-enhancing lesion(s) present at the same time</p>

Table 1.3 McDonald Criteria for diagnosis of multiple sclerosis; adapted from [20]

Clinical Presentation	Additional Data Required
<ul style="list-style-type: none"> • ≥ 2 attacks • Objective clinical evidence of ≥ 2 lesions <p style="text-align: center;">OR</p> <ul style="list-style-type: none"> • Objective clinical evidence of 1 lesion with evidence of prior attack 	None
<ul style="list-style-type: none"> • ≥ 2 attacks • Objective clinical evidence of 1 lesion 	DIS OR Await further clinical attack suggestive of a different site in the CNS
<ul style="list-style-type: none"> • 1 attack • Objective clinical evidence of ≥ 2 lesions 	DIT OR Await second clinical attack
<ul style="list-style-type: none"> • 1 attack • Objective clinical evidence of 1 lesion 	DIS + DIT OR Await further clinical attack
Suggestive of PP MS	<ul style="list-style-type: none"> • 1 year of disease progression <ul style="list-style-type: none"> • 2 of the following: <ol style="list-style-type: none"> a. DIS in brain: ≥ 1 T2 lesion in MS regions b. DIS in spinal cord: ≥ 2 T2 cord lesions c. Positive CSF d. Isoelectric focusing evidence of oligoclonal bands <p style="text-align: center;">AND/OR Elevated IgG index</p>

1.3 Pathogenesis of Multiple Sclerosis

Although the exact mechanisms remain to be elucidated, the clinical features of MS can be attributed to a triad of neural tissue injury processes: inflammation, demyelination, and axonal degeneration [2, 13]. Auto-reactive myelin-specific T-lymphocytes appear to be the main culprits eliciting

demyelination. Activated by molecular mimicry, these lymphocytes initiate a cascade of subsequent events such as blood-brain-barrier disruption, microglial activation, excitotoxicity, plaque development, and ultimately neurodegeneration and microglial scarring [13, 21-23]. Evidence of inflammation can be seen in biopsied plaques, which contain lymphocytes and macrophages, and additionally myelin reactive T-cells are observed in the blood and CSF of MS patients [24-26]. Microglia contribute to the inflammatory atmosphere, instigated by the T-cells, by releasing proteolytic enzymes, cytokines, oxidative products, and free radicals creating an environment that is toxic to oligodendrocytes and myelin [27, 28]. Inflammation elicits demyelination and axonal damage, the process likely underlying permanent neurological impairment and conduction failure. Axonal injury has been recently recognized as playing a critical role in the symptomatic development in MS patients [29-32]. Ultimately, compromise of axons is believed to lead to the neuronal degeneration, cerebral atrophy, and permanent loss of function, all of which are characteristic of late stage MS.

Despite the inflammatory and autoimmune nature of the disease, traditional anti-inflammatory therapies have so far demonstrated marginal effect in lengthening time between relapses, alleviating symptoms long-term, and slowing disease progression [13, 33]. Development of a novel treatment strategy necessitates additional study of pathogenic mechanisms. Establishment of well-defined links between the observed inflammatory reactions, demyelination, and axonal damage will enable identification of more suitable pharmacologic targets.

1.4 Oxidative Stress-Induced Damage to Axolemma and Myelin

Many recent studies suggest that oxidative stress underlies damaging pathological processes of CNS diseases and trauma [34-37]. In part, this can be explained by the inherent vulnerability of the CNS to oxidative stress due to low levels of intrinsic anti-oxidants (catalase and GSH-peroxidase), high composition of polyunsaturated lipids (membrane and myelin), and high quantities of ROS produced by essential neurochemical processes in healthy CNS cells, relative to other organ systems [34-39]. Consequently, in disease states, the CNS is especially susceptible to oxidative insult by reactive oxygen species (ROS) and lipid peroxidation (LPO) byproducts. Until recently, studies have predominantly attempted to reduce oxidative damage in the CNS by pharmacologically targeting ROS to alleviate neurotoxic effects [38, 40-42]. However, this therapeutic approach has yielded inconsistent results in achieving symptomatic improvement in animal models of CNS disease and trauma, leading researchers to target LPO products therapeutically.

1.5 The Neurotoxic Nature of Acrolein

Acrolein, an α,β -unsaturated aldehyde and LPO byproduct, appears to have a crucial role in mediating and perpetuating oxidative stress. Acrolein, produced endogenously by lipid peroxidation and exogenously by burning tobacco, frying in oils and petrol, and combustion of wood and plastic, has been implicated in various diseases such as ischemia, spinal cord injury, respiratory diseases, traumatic injury, chronic pain and neurodegenerative diseases by perpetuating oxidative stress [34, 41, 43-47]. Of LPO aldehydes, acrolein is the most abundant and

reactive. In fact, it has been reported to exceed concentrations of other aldehydes, such as 4-hydroxynonenal, by 40 times and is highly reactive with crucial cell components including phospholipids, proteins, and DNA [48-50]. Additionally, the half-life of acrolein is considerably greater compared to ROS (days as opposed to fractions of a second) [48]. Furthermore, acrolein can act as a catalyst to produce more acrolein and ROS initiating a detrimental cycle of oxidative stress. Taken together, evidence indicates that acrolein is capable of instigating and perpetuating oxidative stress.

In addition to endogenous oxidative processes, exposure to acrolein can also occur by way of an exogenous environmental pollutant such as emissions from petrol combustion, cigarette smoking, manufacturing processes, and frying food [51-55]. This raises the possibility of an additive effect when considering acrolein exposure, potentially rendering individuals with pathologically high levels of endogenous acrolein more susceptible to environmental acrolein, since acrolein, regardless of its source, can exacerbate oxidative stress.

Due to its extended half-life compared to ROS, targeting endogenous acrolein has promising applications in diagnosing, monitoring and treating MS. Many current treatments of MS are geared towards preserving functional loss, suppressing inflammation, and reducing immune response associated with the disease such as 4-aminopyridine (Ampyra), Interferons, Glatiramer acetate (Copaxone), Natalizumab (Tysabri), and Fingolimod (Gilenya). Unfortunately, these drugs are very expensive, especially for uninsured patients. Some acrolein scavenging drugs currently being examined, such as hydralazine, are substantially

less expensive, already FDA approved and have been shown to be effective at both delaying onset and decreasing the severity of symptoms in in vitro and in vivo studies [56].

1.5.1 Acrolein-Mediated Demyelination

Demyelination within the CNS, a main feature of MS development and progression, manifests as a transient functional loss characteristic of RRMS [13, 33]. Loss of myelin structural integrity hinders neuron function by increasing the energy needed for action potential propagation. If myelin is not repaired, adenosine triphosphate (ATP) stores will eventually be depleted and action potential conduction will cease. Acrolein is not only capable of directly damaging myelin but also anchoring proteins that secure myelin to the axon. In the event of damage to an anchoring protein, myelin will split and separate from the axon; a process known as decompaction. In instances where myelin damage is severe and myelin decompaction occurs, voltage-gated potassium (VGK) channels are no longer localized to the juxtaparanodal region but instead aberrantly expressed along the length of the axon. Abberant expression of VGK channels also leads to impairment of action potential propagation due to the unregulated outward current of potassium ions and loss of ionic gradient essential for action potential generation [57-59]. In one ex vivo study, myelin retraction from the nodes of Ranvier and myelin decompaction were observed following isolated spinal cord incubation in acrolein [58]. Furthermore, exposure of juxtaparanodal VGK, absent action potential propagation, and aberrant VGK expression were reported [58, 60].

Previously thought to be separate aspects of the MS pathology, demyelination and axolemma damage now appear to be more related than previously thought; damage to axons and/or myelin can affect ionic gradients and localization of channels along the axon, essential processes in signal conduction [61-64]. Acrolein is capable of affecting both of these neuronal components and therefore is likely a contributor to detrimental processes underlying function deterioration in MS patients.

1.5.2 Acrolein-Induced Axonal Injury in Multiple Sclerosis

Clinical ex vivo studies assessing markers of myelin disruption and axonal damage in MS patient brain tissue were the first to implicate the axonal degeneration as an important mechanism underlying symptoms of MS. The studies revealed a large quantity of transected axons, which could explain permanent neurological impairment seen in late stages of MS [32, 65]. In another study, inflammatory damage to axons led to conduction deficits and emergence of symptoms in animal models and clinical MS cases [32, 66]. Evidence of the critical role of axonal injury in MS, has prompted some to hypothesize that axonal injury resulting in degeneration would elicit a permanent functional deficit like that seen in SP- and PP MS [32, 65].

As stated previously, acrolein can directly injure axolemma, likely due to the phospholipid component. Additionally, demyelination, aside from previously mentioned detrimental effects, renders the axonal membrane vulnerable to the harsh extracellular environment of inflammatory mediators, acrolein and other

highly reactive molecules. In this way, acrolein is capable of inflicting membrane damage both directly and indirectly.

We have shown acrolein exposure compromises the structural integrity of cell membrane and prolonged exposure results in an increase in axon permeability and a halt of compound action potential propagation [41, 67, 68]. Application of acrolein scavenger, hydralazine, proved to be neuroprotective to axons in both in vivo and in vitro spinal cord trauma models. Taken together, there is extensive evidence implicating acrolein as an instigator of axonal damage and ultimately, axonal degeneration [59].

1.5.3 Direct and Indirect Impairment of Mitochondrial Processes by Acrolein

Mitochondrial dysfunction is another mechanism believed to underlie symptoms characteristic of MS compromising energy output and ultimately, if left unchecked, initiating cell death pathways. Damage to myelin and axolemma results in an inward calcium current, subsequently triggering cell death pathways and release of mediators that can directly injure mitochondria [33]. In fact, mitochondria may even be more susceptible to acrolein and ROS than other cellular structures.

Mitochondria generate ATP to support cell survival, growth and function; however the electron transport chain causes the non-pathological generation of ROS. In this way, mitochondrial dysfunction not only affects the amount of ATP supplied to the cell but also directly exacerbates oxidative stress through the release of additional ROS. Thus, in a pathological state, mitochondria are

inherently vulnerable to the inflammatory environment and upon death further promote an oxidative stress and CNS damage [69, 70].

Mitochondrial dysfunction has been elicited by acrolein in cardiac tissue, brain and spinal cord [71-73]. In one study, upon exposure to acrolein, isolated mitochondria depleted glutathione (GSH) and increased ROS levels [71]. The brain relies almost exclusively on GSH as an antioxidant due to intrinsically low levels of catalase, further establishing acrolein as a potent neurotoxin [71]. Furthermore, acrolein is known to directly inhibit function of adenine nucleotide translocase through the binding of cysteine residues, an essential component of the electron transport chain. In this way acrolein is capable of directly injuring mitochondria, halting cellular respiration and perpetuating oxidative stress [71, 74, 75].

CHAPTER 2. NEUROPROTECTIVE ROLE OF ACROLEIN SCAVENGERS IN EAE

2.1 Introduction

The therapeutic utility of scavenging acrolein in EAE was first studied in the Shi laboratory. The study employed the FDA-approved antihypertensive hydralazine, which had been previously demonstrated to effectively scavenge acrolein in vitro at concentrations well below those currently approved for the treatment of hypertension. EAE was induced in female C57BL/6 mice by the subcutaneous injection of myelin oligodendrocyte/compleat Freund's adjuvant at caudal and rostral ends of the mouse spinal cord to elicit an autoimmune response to myelin (Figure 2.1). Deconjugated pertussis toxin was administered intraperitoneally at the time of myelin oligodendrocyte glycoprotein (MOG) application and again 24 hours later to increase blood brain barrier permeability and facilitate immune cell infiltration into the CNS. Hydralazine (1mg/kg) was administered I.P. daily to the treatment group beginning on day of model induction. Behavioral scores were monitored through the conclusion of the study, at which point animals were euthanized and immunoblotting and immunohistochemical techniques were performed to quantify acrolein-lysine adduct level within the spinal cord and myelin integrity, respectively. Acrolein was found at significantly greater

levels in EAE spinal cords when compared to both control and hydralazine-treated groups. Additionally, application of an acrolein scavenger in EAE mice provided a neuroprotective effect, significantly attenuating behavioral deficit and reducing demyelination relative to untreated EAE counterparts. These results demonstrate the potential of acrolein scavenging as an effective therapeutic strategy in combating the detrimental effects of the EAE model and potentially even in the treatment of clinical cases of MS.

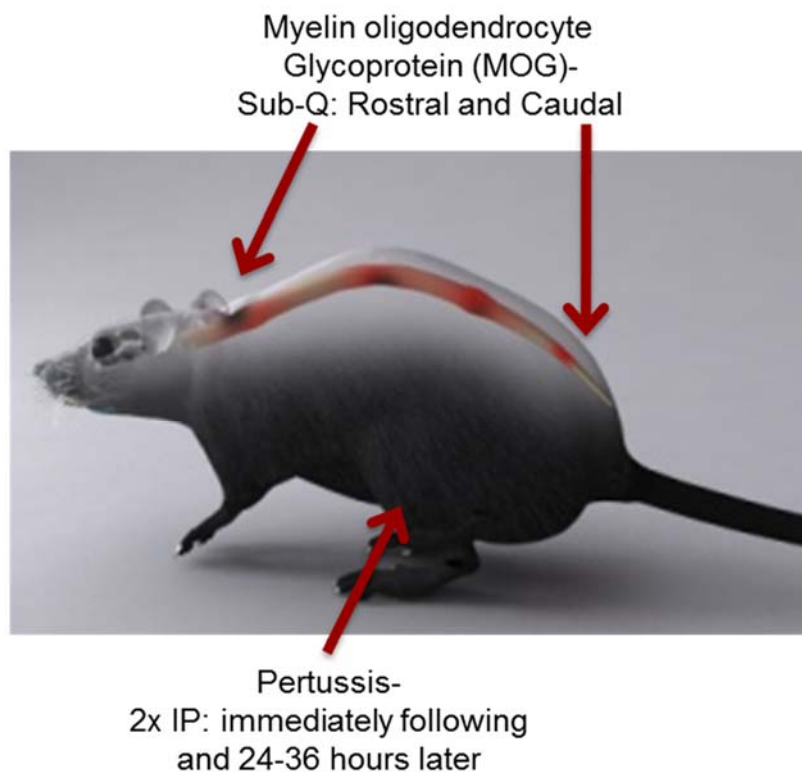


Figure 2.1 Induction of EAE model. C57BL/6 mice were injected subcutaneously with MOG emulsion at rostral and caudal ends of the spinal column. An intraperitoneal injection of deconjugated pertussis toxin was administered at time of MOG injection and, again, 24-36 hours later.

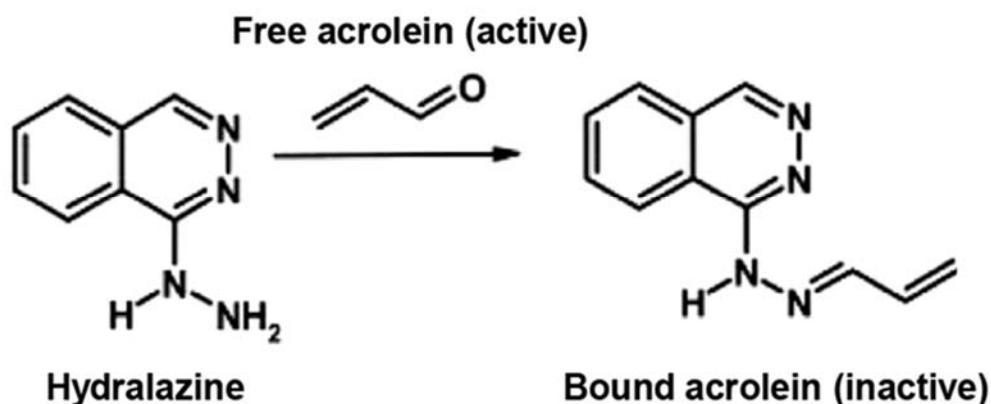


Figure 2.2 Acrolein Scavenging by Hydralazine. Schematic of mechanism by which hydralazine neutralizes acrolein. Acrolein binds to hydrazine group of hydralazine.

2.2 Acrolein-Lysine Adducts Increased in EAE Spinal Cord Tissue

Acrolein-lysine adduct level in the spinal cord was quantified using immunoblotting in three groups: saline-treated control mice (n=3), EAE mice (n=3) and hydralazine-treated EAE mice (n=3). Untreated EAE mice exhibited significantly increased levels of acrolein-lysine adducts (20.27 ± 3.0 a.u.) compared to saline treated control mice (12.30 ± 1.3 a.u., $p < 0.05$, Fig 2.2 B). Hydralazine-treated EAE mice (15.4 ± 1.6 a.u.) also demonstrated a decrease in acrolein-lysine adduct level relative to control, although this difference was not found to be significant.

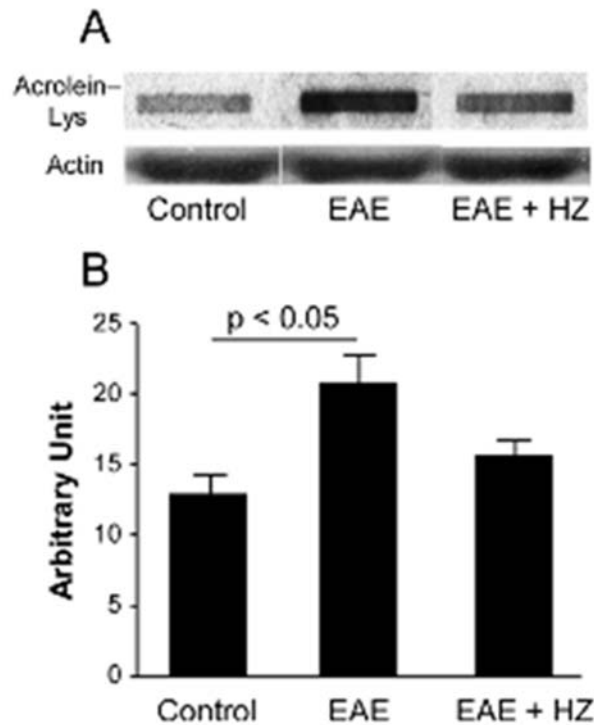


Figure 2.3 Dot Immunoblotting Quantification of Acrolein-Lysine Adducts in Spinal Cord. Immunoblotting demonstrated an increase in acrolein-lysine adduct level in EAE mouse spinal cord. Band intensities were quantified using ImageJ and expressed in arbitrary units. (A) Representative blot for each group. (B) Acrolein-lysine adduct level was significantly increased in untreated EAE mice (20.27 ± 3.0 a.u.) relative to sham-treated control mice (12.30 ± 1.3 a.u., $p < 0.05$). Hydralazine-treated EAE mice exhibited an acrolein lysine adduct level of 15.14 ± 1.6 a.u. Statistical analysis was performed using a one-way ANOVA and post-hoc tests. All data are expressed as mean \pm SEM.

2.3 Hydralazine Attenuated Behavioral Deficit and Myelin Damage in EAE mice

Behavioral assessments of hydralazine-treated and saline-treated EAE mice were performed daily throughout the course of the study using a 5-point behavioral scale (Figure 2.2 A). The average onset of symptoms in the hydralazine-treated group (21.73 ± 2.1 days post-induction) was significantly

prolonged compared to their saline-treated counterparts (15.42 ± 0.4 days post-induction, $p < 0.01$, Figure 2.2 B). Additionally, symptom severity was quantified by averaging the highest scores for individual animals within each group starting. Hydralazine-treated EAE mice (1.72 ± 0.4) demonstrated significantly lower behavioral scores than the saline-treated EAE mice (3.33 ± 0.3 , $p < 0.05$, Figure 2.2 C). For myelin quantification, thoracic spinal cord segments were extracted from saline-treated EAE, hydralazine-treated EAE, and controls, sectioned and stained with fluoromyelin. Control sections did not exhibit signs of demyelination. There was a statistically significant difference in demyelination area between saline-treated ($25.58 \pm 3.8\%$, $n=3$) and hydralazine-treated ($5.10 \pm 4.2\%$, $n=3$, $p < 0.05$) EAE groups (Figure 2.3).

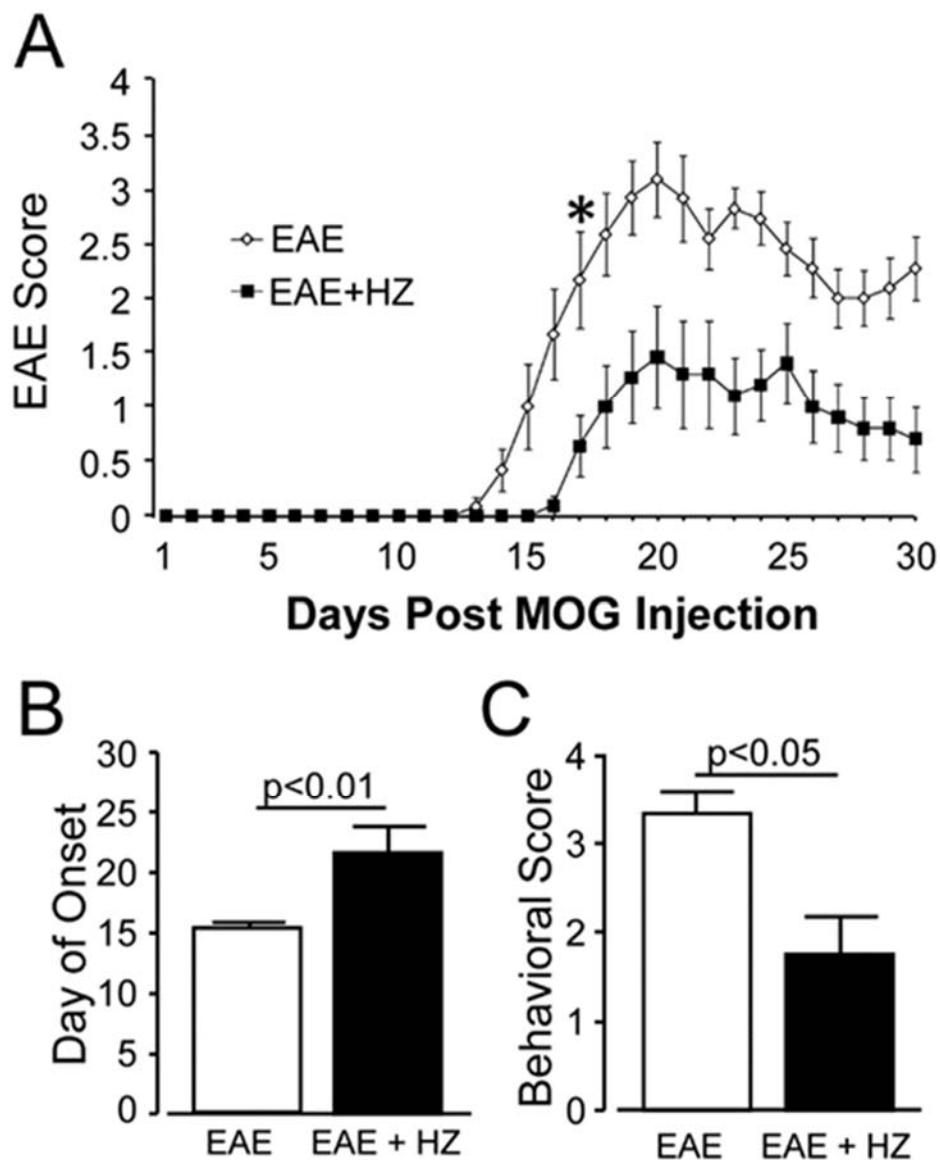


Figure 2.4 Hydralazine Therapy Ameliorated Motor Deficits. (A) Behavioral assessment of saline-treated EAE and hydralazine-treated EAE mice ($p < 0.01$ when groups compared after day 17). (B) Hydralazine treatment delayed symptomatic onset of EAE relative to saline-treated EAE ($p < 0.01$). (C) Mean peak behavioral score was averaged for each group. Hydralazine-treated EAE mice exhibited a significantly lower peak behavioral score ($p < 0.05$).

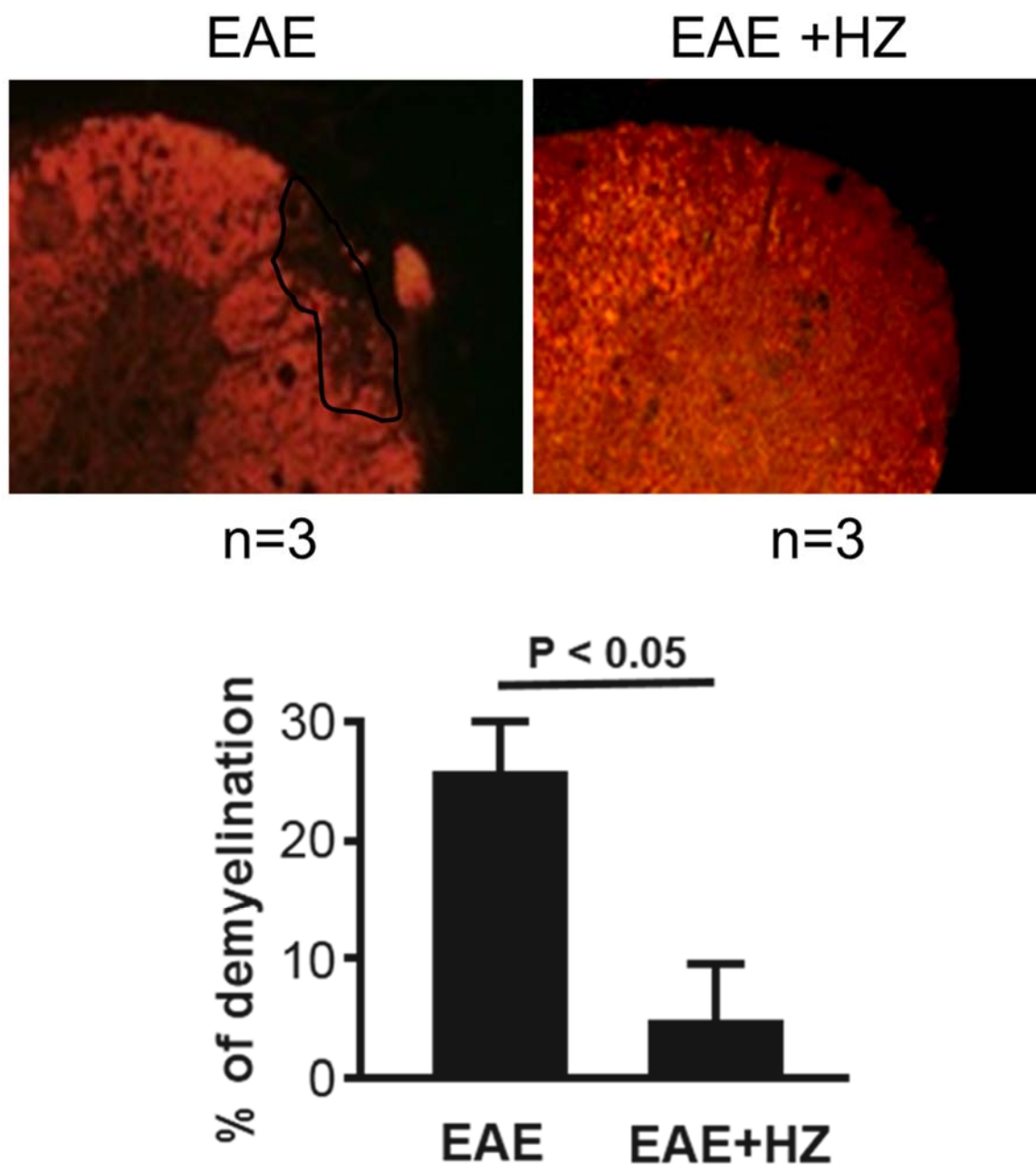


Figure 2.5 Attenuation of Acrolein-Lysine Adducts by Hydralazine Treatment. Immunohistochemical analysis of myelin, using a myelin basic protein (MBP) stain. Quantification was carried out using ImageJ. Spinal cords from the saline-treated EAE group experienced significantly increased demyelination compared to their hydralazine-treated counterparts ($p < 0.05$).

2.4 Application of Hydralazine at Time of Symptom Emergence

Although acrolein scavenging using hydralazine was shown to be an effective neuroprotective strategy in EAE, it is important to note that treatment with hydralazine began at the time of model induction. However in a clinical scenario, a patient would not be treated for a disorder until they present with obvious, diagnosable symptoms. To address this fundamental issue and ascertain the clinical utility of acrolein scavenging, we conducted a study in which mice were not treated with hydralazine until behavioral deficit emerged (score of 1-tail paralysis). Even with delayed application of hydralazine, a neuroprotective effect was still observed, in which rate of symptom progression and behavioral scores were significantly decreased in hydralazine-treated EAE mice relative to their saline-treated counterparts.

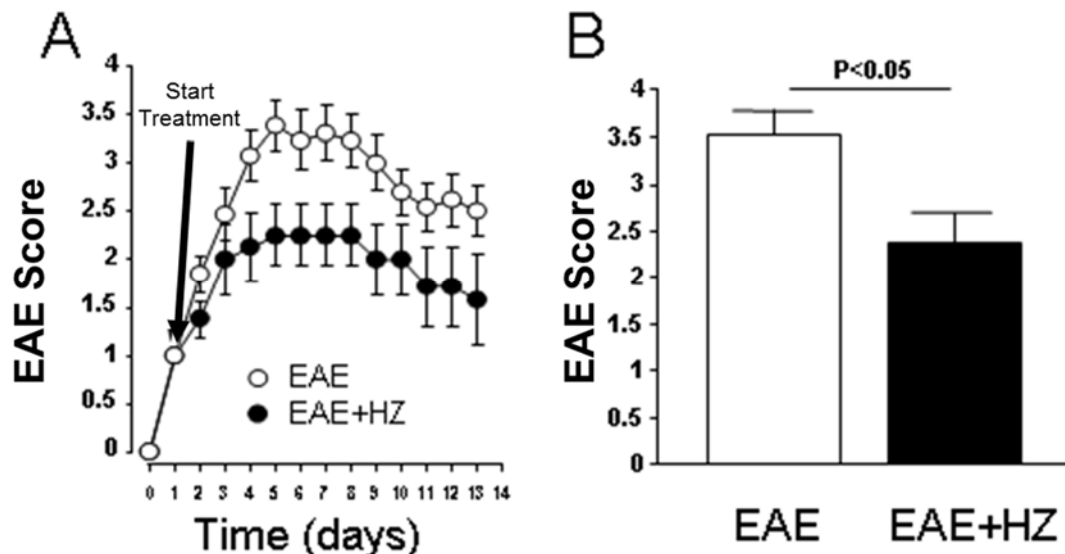


Figure 2.6 Hydralazine Application at Symptom Onset. (Left) Behavioral score of saline-treated EAE mice and EAE mice when treated with hydralazine at symptom onset. Treated mice displayed significantly lower EAE scores than the sham treated group

2.5 Summary and Significance

This study further demonstrated the neurotoxic nature of acrolein and implicated it as a relevant pathologic factor in EAE and likely in MS as well. Acrolein-lysine adducts were detected at significantly increased levels in EAE mice in concordance with emergence of motor deficit. Furthermore, daily administration of acrolein scavenger hydralazine conferred a neuroprotective effect, attenuating, reducing severity and delaying onset of motor deficit in EAE mice when applied at time of model induction through the end of the study. Ex vivo analysis of myelin using immunohistochemistry demonstrated that hydralazine treatment also resulted in a significant reduction in demyelination within thoracic white matter. Additionally, when hydralazine was administered when EAE animals first presented with tail paralysis, the earliest sign of EAE motor impairment, significant reduction in behavioral score was observed in the treatment group. In light of this finding, it is reasonable to suggest the potential of acrolein scavenging for treatment of clinical cases of MS. Treatment application at emergence of symptoms is a more clinically relevant, due to treatment in clinical scenarios beginning when patients present to their physician with a problematic symptom. Hydralazine is an effective scavenger for both acrolein and acrolein-protein adducts and attenuated neurotoxic effects in the EAE model when applied at time of model induction or at emergence of motor deficit. Since hydralazine is already an FDA-approved compound and doses used in this study are safe in humans, therapeutic acrolein scavenging could potentially be employed in the future as a treatment for MS patients with relative ease.

CHAPTER 3. ALLEVIATION OF BEHAVIORAL IN EAE USING ALTERNATIVE ACROLEIN SCAVENGERS

3.1 Introduction

Due to the demonstrated neuroprotective effects of hydralazine treatment in the EAE model, acrolein scavenging has proven to be an effective treatment to improve motor function and delay symptom onset. In order to further establish the therapeutic benefit of scavenging acrolein, it is crucial to demonstrate that the acrolein scavenging capability of hydralazine underlies its therapeutic utility in the EAE model, rather than its currently approved usage as an antihypertensive. As such, two alternative acrolein scavengers, phenelzine, an MAO-I antidepressant, and EGCG, a green tea catechin, were identified as other compounds containing hydrazine groups, the functional group of acrolein scavengers, and evaluated in the same manner as hydralazine.

3.2 Materials and methods

3.2.1 Experimental Autoimmune Encephalomyelitis (EAE) mice

Female C57BL/6 mice were injected with 0.1 mL MOG/complete Freund's adjuvant emulsion (MOG) (Hooke Laboratories, Lawrence, MA) subcutaneously over the caudal and rostral ends of the spinal cord. This mixture mimics endogenous proteins and creates an immune response to myelin in the central nervous system. Immediately following the emulsion injection, 0.1 mL of

deconjugated pertussis toxin, (Hooke Laboratories) which is believed to create a more permeable blood brain barrier and hasten the onset of symptoms, was given intraperitoneally and again 24 hours later.

3.2.2 Behavioral Assessment

Behavioral assessment was performed using a 5-point scale for quantification. Animals were placed on a grate to observe walking ability and motor function. The scale is as follows: 0 – no deficit; 1 – limp tail only; 2 – hind limb paresis without frank leg dragging; 3 – partial hind limb weakness with one or both legs dragging; 4 – complete hind limb paralysis; 5 – moribund, paralysis in hind limbs and forelimbs. The animals were monitored three times for the first week and then daily until the end of the study.

3.2.3 In vivo phenelzine treatment

Phenelzine sulfate salt (Sigma Aldrich) was dissolved in phosphate buffered saline (1x) and then sterilized through a vacuum filter. Intraperitoneal phenelzine treatment (15 mg/kg, 0.1 mL) was initiated at three different time points: day of induction, at behavioral symptom onset (score=1), and at symptom peak (score=3). Control animals received intraperitoneal injections of saline rather than phenelzine.

3.2.4 In vivo EGCG treatment

PBS was bubbled with nitrogen for five minutes before epigallocatechin gallate (Sigma Aldrich, St. Louis, MO) was dissolved at a concentration of 4 mg/mL. Following dissolution, the solution was bubbled further to prevent auto-oxidation. After bubbling, the solution was sterilized using a 0.2 um syringe filter

under nitrogen. Daily treatments of EGCG (20 mg/kg) were administered I.P. at a volume of 0.1 mL, starting on day of induction through the conclusion of study. Control animals received 0.1 mL saline as a sham treatment.

3.2.5 Spinal cord tissue preparation

Animals were anesthetized with a Ketamine (90 mg/kg) and Xylazine (10 mg/kg) and then perfused with cold Krebs solution (124 mM NaCl, 2 mM KCl, 1.2 mM KH₂PO₄, 1.3 mM MgSO₄, 2 mM CaCl₂, 10 mM dextrose, 26 mM NaHCO₃, 10 mM sodium ascorbate) to both lower the body temperature and drain the blood. For immunoblotting, the spinal column was then quickly removed and a complete laminectomy performed. The spinal cord was then excised from the vertebrae and placed in cold oxygenated Krebs solution.

For immunohistochemical analyses, following perfusion with Krebs solution, animals were subsequently perfused with 4% paraformaldehyde. The spinal column was then removed and incubated in 4% PFA for 1 hr. The spinal cords were then extracted from the spinal column and cut into three 2 cm sections: cervical, thoracic and caudal. Spinal cord segments were then incubated in 15% sucrose for 24 hrs and then in 30% sucrose for 24 hrs. Tissue was then embedded and frozen in OCT compound until slicing.

3.3 Phenelzine

Phenelzine is an FDA-approved MAO-I antidepressant that has acrolein scavenging capabilities. In order to further establish acrolein scavenging as a novel therapeutic strategy in EAE and MS, it was critical to demonstrate that two structurally distinct drugs apart from acrolein scavenging groups, were both able

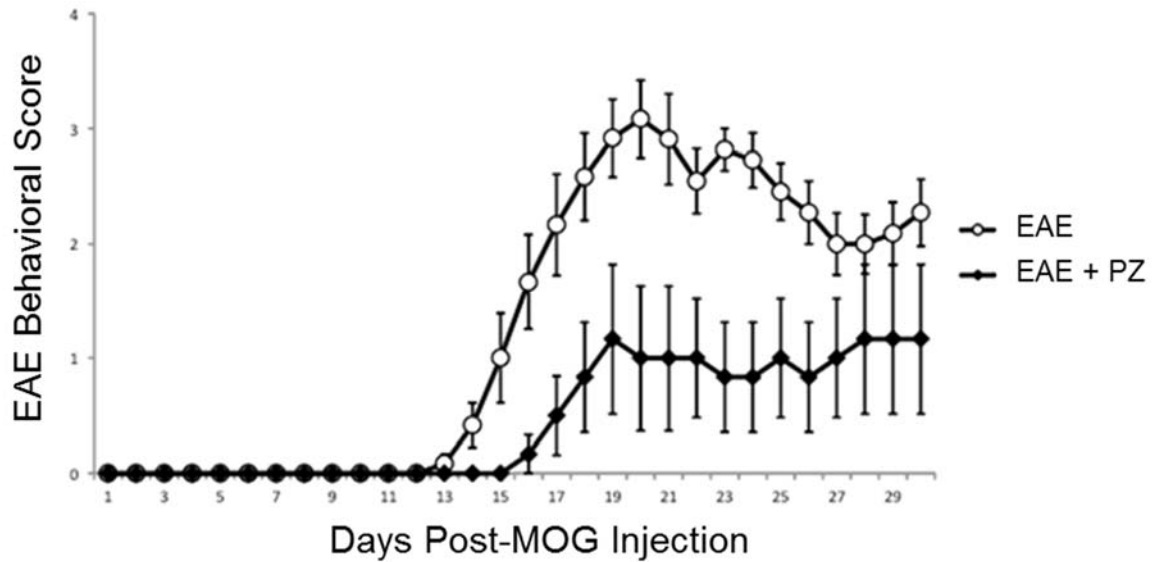


Figure 3.2 Behavioral Assessment of Sham-Treated (n=8) and Phenzelzine-Treated EAE Mice (n=8). Phenzelzine-treated mice demonstrated a delayed onset of symptoms, decreased symptom severity, and slowed symptom progression relative to sham-treated controls ($p < 0.1$).

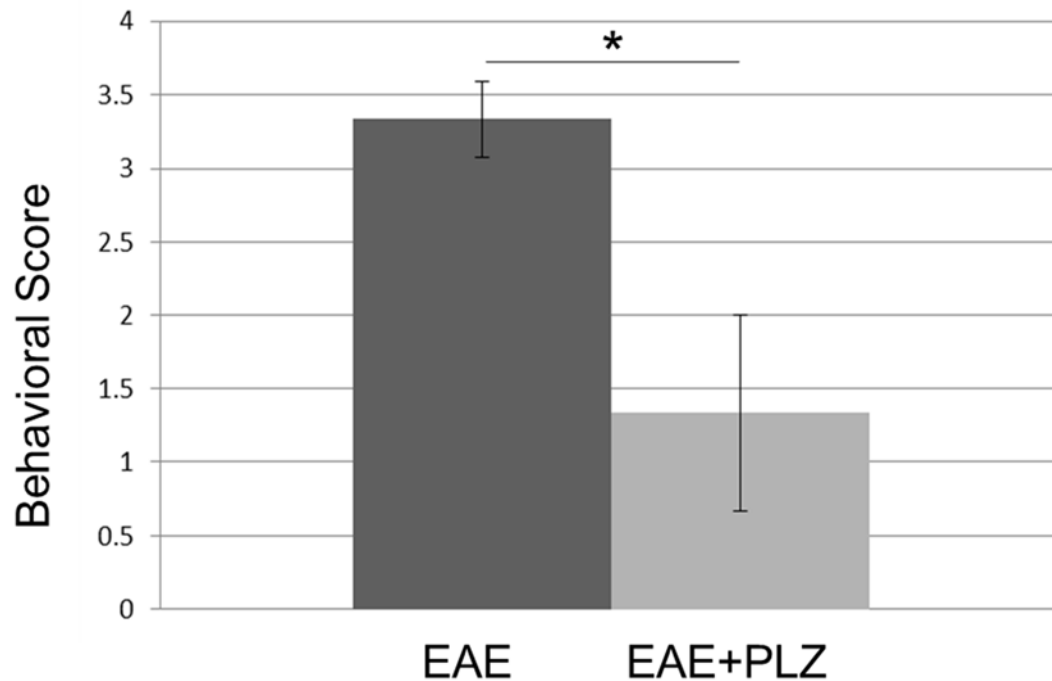


Figure 3.3 Phenzelzine Attenuated Behavioral Deficit in EAE Mice. Treatment with phenzelzine significantly decreased mean behavioral score (1.3 ± 0.7 ; n=6) relative to control sham-saline treated mice (3.3 ± 0.25 ; n=12; $p < 0.005$).

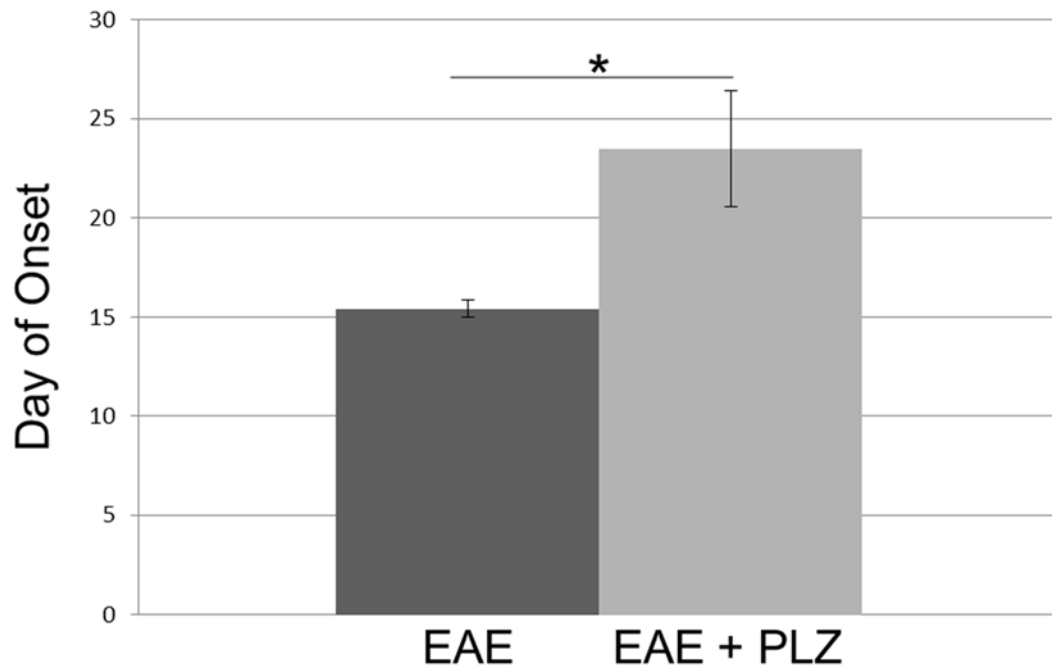


Figure 3.4 Phenelzine delayed Symptomatic Onset in EAE Mice. Phenelzine-treated animals exhibited a significantly delayed onset (23.5 ± 7.2 ; $n=6$) when compared to controls (15.4 ± 2.9 ; $n=12$; $p < 0.001$)

3.4 Epigallocatechin Gallate (EGCG)

EGCG is an antioxidant naturally present in green tea and has been shown to have therapeutic utility in other diseases such as cancer, HIV, and other neurodegenerative diseases. In fact, EGCG has already demonstrated potential as a treatment for MS; however mechanisms through which it exerts its neuroprotective effects have yet to be fully characterized. However, as an antioxidant and acrolein scavenger, EGCG holds great promise as an effective natural compound to combat oxidative stress. In this regard, the current study aims to evaluate the effectiveness of EGCG in alleviating oxidative stress, particularly its ability to mitigate neurodegenerative processes by sequestering acrolein in vivo in

a murine model of MS. Two groups of EAE mice, one sham-treated with 0.1mL PBS and the other treated with 0.1mL of EGCG (20 mg/kg), were subjected to daily behavioral assessment for 28 days. After which mice were euthanized and spinal cords removed for morphological assessment. This study is ongoing, however preliminary behavioral data is presented below. Preliminary results indicate that EGCG has the potential to ease behavioral deficit in EAE mice (Fig 3.2).

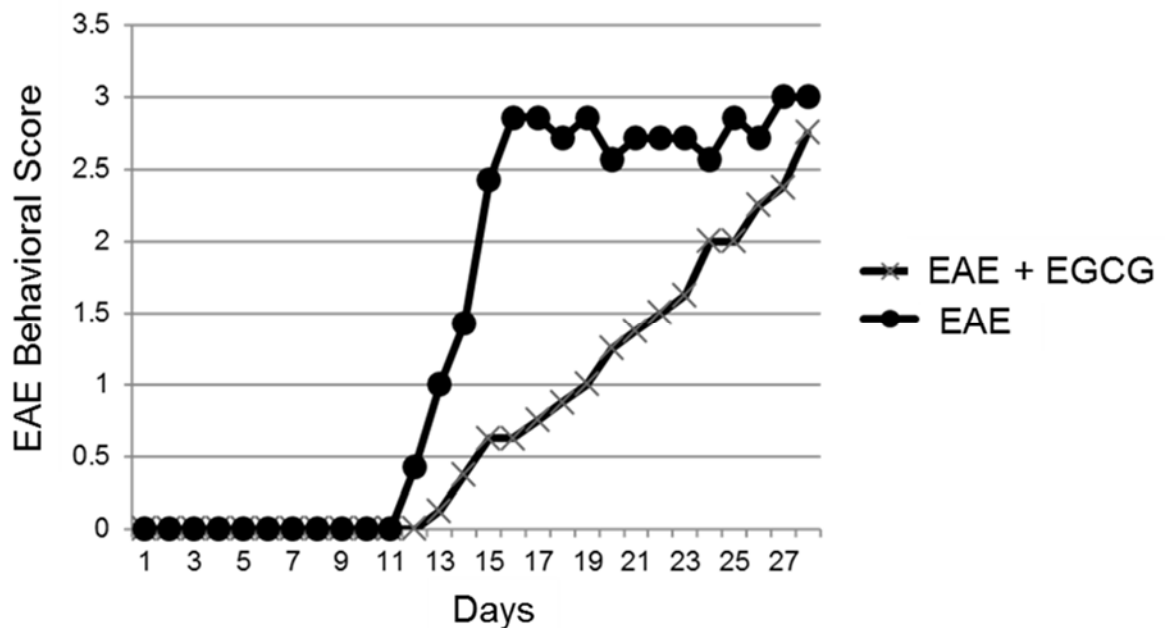


Figure 3.5 Behavioral assessment of sham-treated and EGCG-treated EAE mice. EGCG treatment demonstrates positive preliminary results as an acrolein scavenger, particularly in decelerating disease progression.

3.5 Discussion

In order to further establish acrolein scavenging as a therapeutic approach for the treatment of MS, identification of alternative acrolein scavengers is imperative. The two alternative scavengers identified above, phenelzine and EGCG, performed similarly to hydralazine when applied to improve behavioral outcomes in the EAE model. The commonality of these three compounds lies in the fact that they each contain a hydrazine group(s), which is the component responsible for the binding and neutralization of acrolein. As such, this evidence indicates that the therapeutic benefit of hydralazine in the initial study can indeed be attributed to its acrolein scavenging properties.

CHAPTER 4. APPLICATION OF POLYETHYLENE GLYCOL (PEG) AS A MEMBRANE REPAIR AGENT

4.1 Introduction

It is widely accepted that inflammation is the primary component of the MS pathology, however the exact mechanisms which instigate CNS damage remain incompletely characterized [13, 33]]. Although demyelination is considered the prominent pathologic feature underlying symptom development in MS patients, recent studies indicate that axonal injury and subsequent degeneration also contribute to loss of conduction [2, 76]. These observations indicate that injury to either myelin or axon could potentially manifest as neurological deficits characteristic of MS. Furthermore, axonal degeneration has been suggested as the underlying cause for the transition from RR MS to SP MS due to the fact that this type of damage is irreversible, preventing complete remission following a relapse [77]. This theory is supported by marginal success of therapies directed solely at myelin preservation, particularly in more advanced stages of the disease [13].

In light of these findings, it is critical to further elucidate the role of axonal damage in MS and to explore therapeutic strategies aimed at neuronal protection or repair. Specifically, the cellular processes that are responsible for initiating axonal degeneration remain insufficiently characterized. Previously, our lab demonstrated that traumatic insult to axonal membrane is capable of prompting

axonal degeneration in a spinal cord injury model [78-80]. Interestingly, acrolein, known to play a role in myelin degradation observed in EAE, is also capable of reacting with lipid in the axonal membrane, eliciting damage, and disrupting the structural integrity of the axolemma [41, 46, 68, 81]. As such, we postulate that acrolein could be a pathological factor underlying axonal membrane damage, ultimately leading to axon degeneration and functional loss in MS.

To rescue axons with damaged axolemma, PEG, a hydrophilic bioinert polymer capable of sealing membrane and promoting cell survival, was administered intraperitoneally [82-84]. In another study, PEG effectively restored axolemmal integrity in an animal model of spinal cord injury [84-86]. Despite its promise in treatment of traumatic CNS injuries, PEG has yet to be investigated as a therapy in other disease in which axolemma damage is indicated, such as MS. PEG has the potential to rescue damaged axons within the CNS and consequently prevent neurodegeneration. In order to evaluate the therapeutic potential of PEG in EAE, first it is crucial to establish that axon damage occurs in EAE and corresponds with functional deficit. Once this is confirmed we will proceed to evaluate the therapeutic benefit of PEG by evaluating motor function in EAE mice and assessing membrane permeability following spinal cord extraction. If successful, this study could provide a whole new avenue in the treatment of MS and other diseases in which axonal injury and degeneration are implicated.

4.2 Materials and methods

4.2.1 Experimental Autoimmune Encephalomyelitis Mice

See 3.2.1

4.2.2 Horseradish Peroxidase Exclusion Test

Mice were divided into 4 groups: healthy control mice, PEG-treated EAE mice EAE mice prior to onset of symptoms, and EAE mice exhibiting peak symptoms. Behavior was monitored daily as previously described and at the study conclusion animals were anesthetized with Ketamine (90 mg/kg) and Xylazine (10 mg/kg) and perfused with oxygenated Krebs's solution [56]. The spinal columns were removed and the spinal cords were excised by performing a complete laminectomy. The excised spinal cord was then incubated in a solution of cold, oxygenated Krebs solution and 0.015% horseradish peroxidase (Sigma Type IV, Sigma Aldrich) for two hours. The spinal cords were then fixed at room temperature in 2.5% glutaraldehyde and phosphate buffer for four hours. Post-fixation, 30 μm sections of the tissue were cut using a Vibratome (Electron Microscopy Science, Hatfield, PA, USA). Then the tissue was incubated in a diaminobenzidine solution to visualize HRP uptake through injured axolemma. Using a microscope and computer, images of the stained spinal cord sections were acquired. With the use of ImageJ analysis stained axons were tallied and conveyed as density (axons/ mm^2) [78, 79, 81, 86].

4.2.3 Polyethylene Glycol Treatment and Preparation

A 30% solution of polyethylene glycol (295906, Sigma Aldrich, St. Louis, MO, USA) in phosphate buffered saline was made and subsequently filtered for

sterilization. A volume of 0.1 mL was administered intraperitoneally daily starting from the day of model induction. Control animals received a sham saline injection in lieu of PEG.

4.3 Results

4.3.1 Axonal Membrane Damage and Its Alleviation by PEG in EAE Mice

Using the HRP-exclusion assay, we first assessed the degree of axonal membrane damage in the spinal cords of EAE mice: control mice, EAE mice before symptom onset, EAE mice at peak behavioral deficit, and PEG-treated EAE mice. The average HRP labeling for these conditions was 867 ± 172 axons/mm², 3337 ± 719 axons/mm², 6510 ± 957 axons/mm² and 1602 ± 357 axons/mm², respectively (Fig 4.1). Both pre-symptom and peak-symptom mice exhibited significantly increased HRP uptake relative to healthy controls ($P < 0.05$; $P < 0.05$). In order to ascertain whether PEG can effectively repair the injured axolemma, EAE mice were treated daily with 0.1 mL 30% PEG and treatment was initiated on day of model induction. Interestingly, we have determined that PEG treated animals demonstrated significantly lower HRP uptake than the peak deficit EAE group.

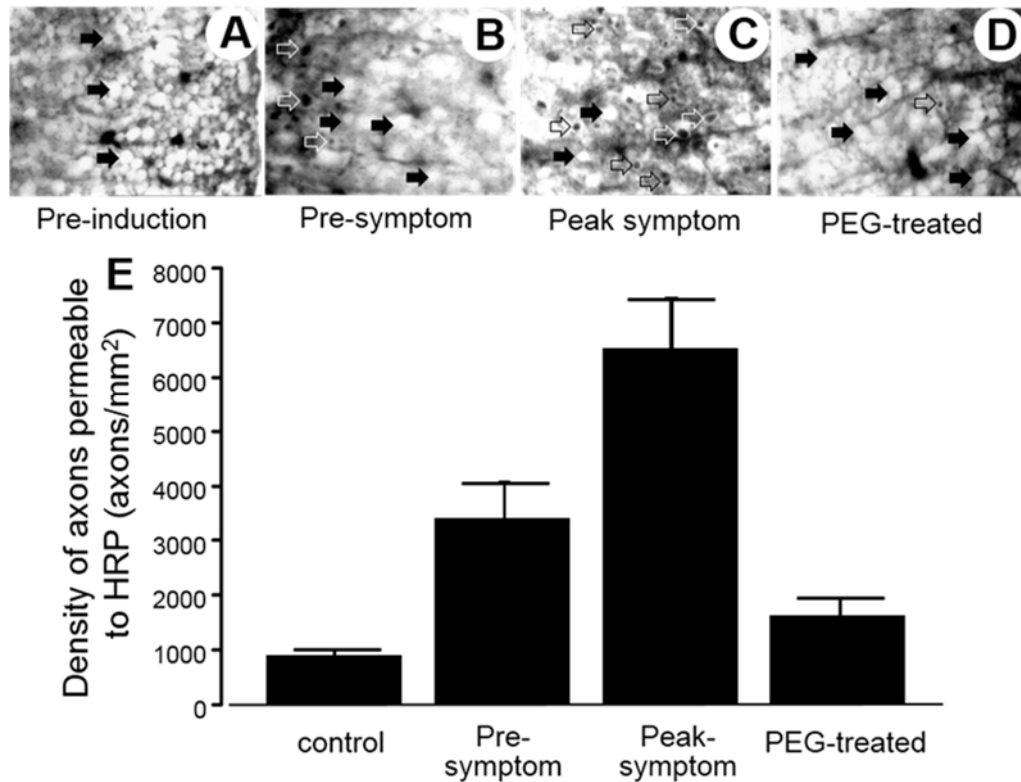


Figure 4.1 Axonal Membrane Damage in EAE and its Alleviation by PEG. Horseradish peroxidase (HRP)-exclusion test determined amount of axonal membrane damage in healthy control mice (n=3), pre-symptom EAE mice (n=5), peak symptom EAE mice (n=4), and PEG-treated mice (n=5). A-D) The images represent HRP-stained sections of spinal cord tissue from the four groups. Solid arrows denote areas in which HRP did not penetrate the cell while the open arrows point to areas depicting HRP penetration revealing increased axonal membrane permeability. E) The bar graph quantifies HRP uptake in each group. The value for control group is 867 ± 172 axons/mm². The peak symptom group had the highest levels of axonal damage (6510 ± 957 axons/mm², $P < 0.05$ compared to control) while the pre-symptom group exhibited increased levels compared to the control group (3337 ± 719 axons/mm², $P < 0.05$ compared to control). The HRP labeling in the EAE/PEG-treated group (1602 ± 357 axons/mm²) is significantly lower than EAE group ($p < 0.05$).

4.3.2 PEG Treatment Significantly Reduced Symptom Severity and Delayed Disease Onset in EAE mice

In order to ascertain the effectiveness of PEG treatment, behavioral scores from two experimental groups EAE and PEG-treated EAE were compared. Behavioral scores for each animal were recorded daily for 4 weeks as previously described [56]. Figure 4.2 demonstrates the relationship between average behavioral score over time for the two groups. The EAE mice that received PEG treatment demonstrated significantly lower behavioral score when compared to their untreated counterparts during days 16 to 25. The mean of the peak scores for each animal were then calculated and PEG-treated EAE mice demonstrated significantly lower mean peak score (1.91 ± 0.4) than the EAE mice (3.33 ± 0.3 , $P < 0.005$) (Fig 4.2 inset).

Furthermore, PEG application also delayed the onset of EAE symptoms (Figure 4.3 inset). Sham treated EAE mice, experienced symptomatic onset as expected, between days 13 and 18, while the PEG-treated EAE mice tended to develop initial symptoms at a later time point, as indicated by a delayed mean time of symptom onset. Specifically, five PEG-treated animals developed between days 13 and 18 (similar to sham treated group), three experienced an onset between days 20 and 26, and three mice did not develop symptoms during the entire four week observation period (for averaging purposes day of onset for these animals was recorded as day 28). The mean day of symptomatic onset in PEG-treated EAE mice was 20.63 ± 1.8 days, which was delayed significantly relative to sham-treated EAE mice (15.42 ± 0.4 days, $P < 0.05$) (Fig 4.2).

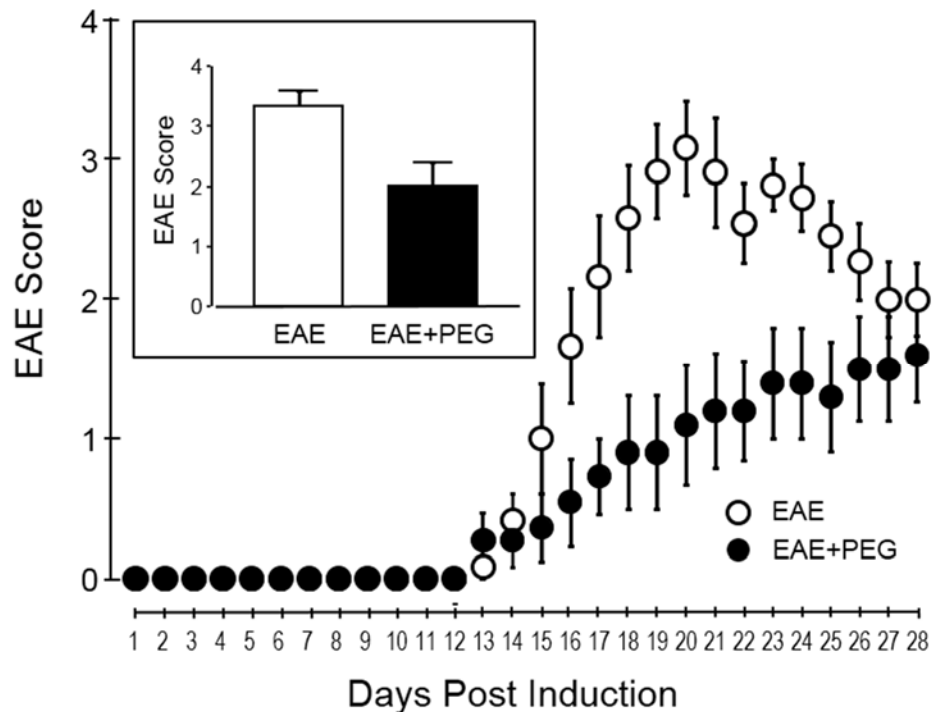


Figure 4.2 Evaluation of PEG as a Therapy for EAE Axonal Damage. Comparison of behavioral assessment each day between EAE (n =12) and PEG-treated (n=11) groups. The graph represents the average score for each group of animals throughout the study. The inset demonstrates that administration of PEG significantly decreased the severity of symptoms in EAE mice ($P < 0.005$). The highest score of each animal was recorded and averaged within each group to quantify the mean score of severity to be used for the inset.

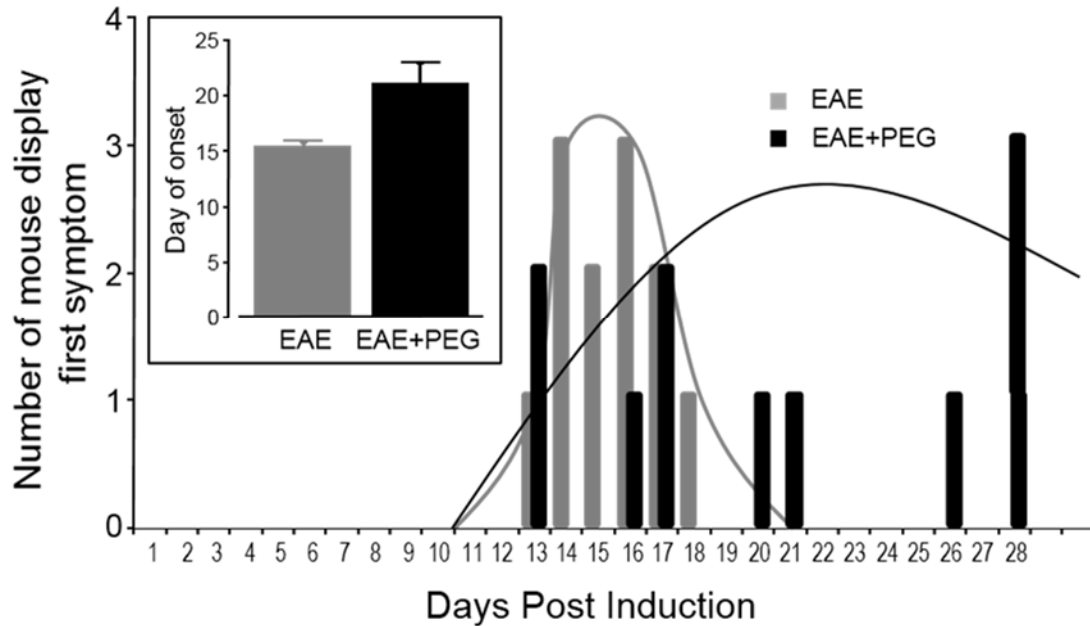


Figure 4.3 PEG Delayed Symptom Onset in EAE Mice. Comparison of onset of symptoms between EAE (n=12) and PEG-treated (n=11) groups. The graph represents the temporal distribution and the day of onset of symptoms between EAE and PEG-treated mice. On the first day symptoms appeared, the number of mice in each group was recorded. The EAE mice were tightly clustered together earlier in the study while the PEG-treated mice were more dispersed. The inset graph represents the average day of onset for EAE and PEG-treated groups.

PEG-treated animals developed symptoms significantly later in the study compared to EAE mice ($P < 0.01$). Three mice in the PEG-treated group never developed symptoms and were counted as day 28 for both graphs.

4.4 Discussion

Using the HRP-exclusion assay to quantify axolemma permeability, we have verified axonal membrane damage is greatest when symptoms are at their peak severity [78, 79, 86]. Also, although not as robust, axonal membrane permeability was significantly increased even in pre-symptomatic EAE mice, indicating that axonal membrane damage is indeed a critical component underlying the development of EAE (Fig 4.1).

Furthermore, the daily application of the membrane sealing agent PEG, elicited a significant reduction in axolemma injury as indicated by decreased membrane permeability following the HRP assay relative to the sham-treated group (Fig 4.1) [84, 85, 87]. Along with the neuroprotective effect afforded to axons, PEG treatment also delayed symptomatic onset and reduced severity of behavioral deficit (Fig 4.2, 4.3). In light of these findings, it is evident that axolemma injury is a critical component of the EAE pathology and partly underlies functional impairment. Additionally, we have identified a way to repair damaged axons using PEG to facilitate membrane resealing, prevent neuronal loss and ameliorate behavioral deficit characteristic of EAE.

These results suggest that administration of PEG to EAE mice is neuroprotective due to its ability to repair axolemma *in vivo*, effectively promoting cell survival and reducing the risk of axon degeneration [2, 76, 88]. Membrane integrity is critical to the maintenance of ionic gradients necessary for generating action potentials and to prevent the influx of calcium into the cell [79, 89, 90]. It is hypothesized that membrane repairing agents also have the potential to curtail mitochondrial dysfunction seen in MS by way of preventing noxious compounds from entering the cells, disrupting the electron transport chain and perpetuating oxidative stress. In this way PEG is neuroprotective in EAE mice through both direct and indirect mechanisms [41, 46, 82, 87, 91, 92].

We also observed a significant degree of increased membrane permeability in pre-symptomatic mice that were subjected to HRP analysis seven days before the emergence of symptoms. Therefore, axonal membrane injury processes

precede the onset of motor deficit by at least seven days. The preservation of motor function despite evidence of significant axonal membrane damage in EAE mice can be attributed to the plasticity of the nervous system. Since there appears to be a certain degree of axon loss associated with symptomatic onset, there is potential to use axonal membrane damage markers to determine when symptoms will emerge.

Since application of PEG promotes axonal membrane resealing, it is feasible to suggest its synergistic use with other therapeutic approaches such as immunosuppression and alleviation of oxidative stress. Due to the link between myelin, axolemma and mitochondrial damage underlying this pathology, it may prove beneficial in employing therapeutic strategies to address both demyelination and axonal membrane damage, both of which will indirectly protect CNS mitochondria from insult by extracellular compounds. The potential success of using PEG in combination with an immunosuppressant or acrolein scavenger can be attributed to PEG's ability to repair existing damage coupled with another compound aimed at removing key mediators of inflammation and oxidative stress.

CHAPTER 5. ESTABLISHMENT OF ACROLEIN DETECTION METHODS

5.1 Introduction

Given the aforementioned evidence of the neurotoxicity and pathological role of acrolein in MS, development of new methods of monitoring acrolein in vivo is crucial if acrolein research is to be translated to a clinical setting. Success in this endeavor could also potentially facilitate the establishment of acrolein as a biomarker for diagnosis, guiding treatment regimens and monitoring relapses by elucidating dynamics of acrolein levels in different phases of MS. Recent advancements have been made in acrolein detection enabling quantification of systemic acrolein levels through the evaluation of a urine or serum sample. The following sections serve as a brief overview of currently available acrolein detection techniques.

5.1.1 Gas Chromatography (GC) and Liquid Chromatography/Mass Spectrometry (LC/MS)

Acrolein detection research began with studies conducted in the 1960s which primarily consisted of studies of environmental pollution and exposure to pollutants [93]. Acrolein exposure by way of pollutants such as car exhaust, industrial processes and cigarette smoke occurs on a much larger scale than endogenous exposure following disease or trauma, allowing for the direct quantification of acrolein with gas chromatography (GC) or liquid chromatography

followed by mass spectrometry (LC/MS) and subsequent derivatization steps [94-96]. While suitable for exogenous exposure studies, GC and LC/MS-based techniques are not the preferred method for endogenous acrolein detection, primarily due to the highly reactive nature and substantially lower concentrations of acrolein [49].

5.1.2 Antibody Detection of Acrolein-Protein Adducts

Considerable developments in endogenous acrolein detection were made by Uchida and colleagues, who introduced acrolein-protein adduct antibodies and enabled quantification of small changes in endogenous acrolein levels [97]. When used in conjunction with Western blotting, these antibodies afford insight into the interactions of acrolein with different proteins. However this method is not preferred when endogenous acrolein is present extremely low concentrations; in this situation dot immunoblotting is employed [44, 98].

The advantage of dot immunoblotting lies in the ability to enhance signal strength by combining all detected acrolein-protein adducts into one focus [56, 98]. The increased sensitivity afforded by this technique, renders it ideal for quantification of acrolein produced by endogenous processes. Additionally, accuracy is also improved in this technique due to simultaneous analysis of artificial acrolein standards and samples. In relation to the current study dot immunoblotting is the preferred method for the assessment of CNS acrolein levels in animal studies.

It is important to note that although these techniques are useful in a preclinical research setting, their clinical applicability is not feasible. This can

primarily be attributed to the highly invasive nature of antibody-based techniques since a biopsied sample of the tissue of interest is required.

5.1.3 3-Hydroxypropyl Mercapturic Acid (3-HPMA) detection with LC/MS/MS

The pursuit of new acrolein detection techniques is vital if acrolein research is to be translated to a clinical setting, as there is a need for minimally invasive techniques to conduct a thorough investigation of the role of acrolein in clinical cases of MS. One of the most promising emerging acrolein detection strategies is the 3-hydroxypropylmercapturic acid (3-HPMA)-based method [99, 100]. This approach is contingent upon the quantification of an acrolein metabolite in either a urine or serum sample of a patient. Level of 3-HPMA, a unique acrolein-GSH metabolite, is indicative of systemic acrolein levels [101]. The main advantage of this approach centers around noninvasive nature, when using a urine sample or its minimally invasive nature, for serum samples [100]. Furthermore, 3-HPMA quantification techniques utilize LC/MS/MS, presenting the possibility for automation and miniaturization for ease of use in clinical acrolein detection [102].

The main disadvantage of this technique is that it does not offer insight as to the cause of an increase in acrolein levels since it is a systemic quantification. Also when GSH is inadequate, as it is in many instances of CNS disease and trauma, 3-HPMA may not reflect the true acrolein level since there is not a sufficient amount of glutathione for acrolein to react with to yield 3-HPMA. This notion is supported by a study conducted by Shi and colleagues in which as higher dosages of acrolein were administered to SCI rats, GSH was consumed and a decline in 3-HPMA level was observed [56, 100]. Additionally, since acrolein can react with a

wide variety of biomolecules, not only GSH, 3-HPMA quantification strategies could potentially underestimate actual systemic acrolein levels.

5.1.4 Translational Nature of Acrolein Research

Due to recent advances in acrolein detection techniques, minimally invasive quantification of systemic acrolein levels can be achieved through the measurement of 3-HPMA, a specific acrolein-glutathione metabolite, in urine and serum using LC/MS/MS. In contrast to previous methods utilized exclusively in animal studies, which required animal euthanization to harvest fresh CNS tissue, this approach allows for the longitudinal assessment of acrolein levels and thus facilitates the translation of acrolein research to clinical scenarios. Collectively, this evidence suggests the potential of acrolein as not only a therapeutic target for MS patients, but also as a biomolecule that could potentially be monitored to aid in diagnosis, predict disease course, and guide treatment regimens on a patient-by-patient basis.

5.2 Materials and methods

5.2.1 Animal Preparation

Rodent studies were conducted in accordance with guidelines mandated by the Purdue Animal Care and Use Committee at Purdue University, West Lafayette, IN, USA. Eight-week-old C57BL/6 female mice (Harlan Laboratories, Indianapolis, IN, USA) were maintained in laboratory animal housing facilities for two weeks prior to EAE induction to minimize potential effects of stress.

5.2.2 EAE Model Induction and Behavioral Assessment

See 3.2.1 and 3.2.2

5.2.3 Dot Immunoblotting

Spinal cords were harvested from mice following exsanguination and perfusion of oxygenated Krebs's solution as described in prior publications. The fresh tissues were incubated with 1% Triton solution and Protease Inhibitor Cocktails, (Sigma-Aldrich, Product #: P8340) homogenized (Kontes Glass Co.) and incubated on ice for at least 1 hour. Samples were then centrifuged at 13,500 g and 4 °C for a minimum of 30 minutes.

BCA protein assay was performed to ensure equal loading for all samples. Samples were transferred to a nitrocellulose membrane using a Bio-Dot SF Microfiltration Apparatus (Bio-Rad, Hercules, CA, USA). The membrane was blocked for 1 h in blocking buffer (0.2% Casein and 0.1% Tween 20 in PBS) and transferred to a solution where polyclonal rabbit anti-acrolein antibody (Novus Biologicals) was dissolved, with a ratio of 1:1000, in blocking buffer with 2% goat serum and 0.025% sodium azide, for 18 h at 4 °C. The membrane was then washed blocking buffer and incubated for 1 hr in a solution of 1:10,000 alkaline phosphatase conjugated goat anti-rabbit IgG (VECTASTAIN ABC-AmP Kit). Final washes of the blocking buffer followed by 0.1% Tween 20 in Tris-buffered saline were performed before the membrane was exposed to substrate of the ABC-AMP kit and visualized by chemilluminescence. Band density was quantified using Image J (NIH) and expressed as arbitrary unit.

5.2.4 Animal Urine Collection

Mice were housed in metabolic cages, designed to obtain urine samples, for 12-24 hours. Regular food and water were supplied during the sample collection period. Samples of approximately 500 µl were obtained from each animal at peak behavioral deficit between days 21-23. Samples were then transferred to 1 ml centrifuge tubes and frozen at -80 °C until biochemical analyses were performed.

5.2.5 Subject Enrollment

All human specimens were collected at the Department of Neurology, Indiana University School of Medicine, Indianapolis, IN, USA by Dr. David Mattson and colleagues. Criteria for subject selection consisted of an MS diagnosis provided that the patient was not be receiving corticosteroids at the time of the sample collection. In this regard, it is important to note that many patients were on various FDA-approved MS immunotherapies at the time of sample collection. This study was carried out in accordance with guidelines set forth in the protocol approved by the Indiana University Human Subjects Institutional Review Board.

5.2.6 Clinical Urine Collection

Subjects were provided with a specimen cup, without preservative, for urine sample collection. Urine samples were then pipetted into labeled cryovials and immediately stored at -70 °C prior to being transported to Purdue University on dry ice. Upon arrival, samples were immediately stored at -80 °C until analysis.

5.2.7 Clinical Serum Collection

Venous blood samples were then obtained (BD Vacutainer® Safety-Lok™ Blood Collection Set 23, Gauge 3/4 Inch Safety Needle, 12 Inch Tubing Sterile) and directly placed into a BD Vacutainer® Plus Venous Blood Collection Tube Serum Tube Clot Activator 13 X 100 mm 6 mL BD Hemogard™ Closure Plastic Tube. Following collection, samples were incubated for 15 minutes at room temperature to facilitate clotting. The samples were then centrifuged at 2800 rpm for 15 minutes (Beckman GS-6R) and transferred to a labeled cyrovial and stored at Thermo Scientific -70 °C. Samples were then transported to Purdue University on dry ice and stored at -80 °C until analysis.

5.2.8 3-HPMA Quantification Using LC/MS/MS and standard preparation

3-HPMA was quantified in urine according to Eckert et al (Eckert, Drexler et al. 2010). Solid phase extraction with Isolute ENV+ cartridges (Biotage, Charlotte, NC) was used to prepare each sample before LC/MS/MS analysis. Cartridges were conditioned with 1mL of methanol, 1mL of water, and 1mL of 0.1% formic acid in water in succession. Urine or serum sample aliquots of 500 µL were combined with 200 ng of deuterated 3-HPMA (d3-3-HPMA) (Toronto Research Chemicals Inc., New York, Ontario), 500 µL of 50 mM ammonium formate and 10 µL of undiluted formic acid and pipetted into the prepared ENV+ cartridges. The cartridges were then washed twice with 1 mL of 0.1% formic acid and 1 mL of 10% methanol/90% 0.1% formic acid in water in succession. The cartridges were dried with nitrogen gas and subsequently eluted with three volumes of 600 µL methanol + 2% formic acid which were combined and dried in a rotary evaporation device.

Samples were reconstituted in 100 μ L of 0.1% formic acid prior to LC/MS/MS analysis.

Quantification of 3-HPMA in the samples was determined using an Agilent 1200 Rapid Resolution liquid chromatography (LC) system coupled to an Agilent 6460 series QQQ mass spectrometer (MS) and a Waters Atlantis T3 2.1mm x 150mm, 3 μ m column for LC separation. Water + 0.1 % formic acid and acetonitrile + 0.1% formic acid were used as buffers. The peak retention time of 3-HPMA/d3-3-HPMA was 6.8 minutes. Multiple reaction monitoring was used for MS analysis. A more detailed procedure is outlined in previous publication (Zheng 2013).

Creatinine quantification was performed to provide an internal standard normalize urine 3-HPMA measurements. Sample creatinine concentrations were determined through the use of a urinary creatinine assay kit (Cayman Chemical Company, Item No. 500701). Urine samples were diluted for 12x and 24x prior to measurement and alkaline picrate solution was prepared following the procedure delineated in the assay manual. The diluted samples and creatinine standards were then loaded into a 96 well plate and incubated with the alkaline picrate solution at room temperature for 20 minutes. Absorbance at 490-500 nm was determined using a standard spectrophotometer and the results were recorded as the initial reading. Following the initial reading, 5ul of acid solution was added to each sample and incubated on a shaker at room temperature for an additional 20 minutes. A spectrophotometer (absorbance at 490-500 nm) was used again to determine the final reading following addition of the acid. The differences between the initial and final absorbance measurements were used for quantitative analysis.

BCA assessment was used as a normalization factor for the serum 3-HPMA measurements. Protein concentrations using bovine serum albumin were quantified using the Bicinochonic Acid protein assay kit (Pierce, Rockford, IL, USA). Serum samples were prepared in a 1:100 dilution and loaded into a 96 well plate along with BCA standards in triplicates. BCA reagent was then added to all wells and the samples were incubated at 37 C for 30 minutes. Following incubation the absorbance of the samples at 560-570 nm was determined using SPECTRAMAX (Molecular Devices, Sunnyvale, CA, USA).

5.3 Results

5.3.1 CNS and Systemic Elevation of Acrolein in EAE Mice

Urine was collected from EAE mice (n=9) and controls (n=9) when peak deficit occurred at days 21-23 (Fig 5.1).

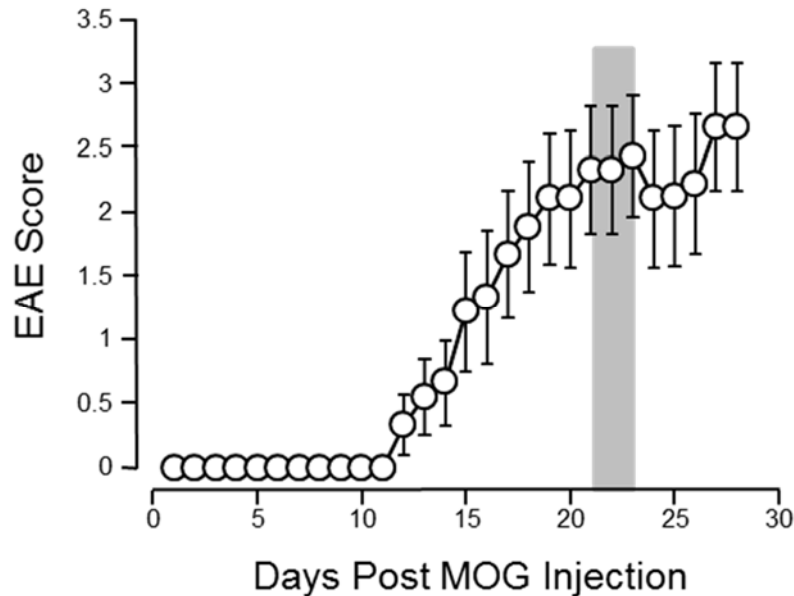


Figure 5.1 Behavioral Deficits Following MOG EAE Induction. The motor deficits typical of EAE were scored daily for 4 weeks. The average value (and SEM) is plotted against time post induction. The shaded area indicates the time period when urine 3-HPMA were collected and assessed using LS/MS and acrolein-lysine adduct of spinal cord tissue were used through dot blot, both assessing acrolein levels. Note the steady rises of EAE score beginning at around 11-12 days and reaches peak around 21-22 days post induction. Data expressed as average \pm SEM.

Systemic acrolein levels were determined through the quantification of 3-HPMA in urine samples using LC/MS/MS. EAE mice demonstrated significantly elevated urine 3-HPMA levels relative to their healthy counterparts (Fig 5.2). Both groups were sacrificed at day 28 and spinal cord tissue was harvested to assess local acrolein concentrations within the CNS using an immunoblotting assay. Measurements of acrolein in the CNS corresponded to the results obtained from 3-HPMA analysis of the urine, in which EAE mice exhibited significantly elevated intrinsic levels of acrolein-lysine adducts relative to the control group (Fig 5.3).

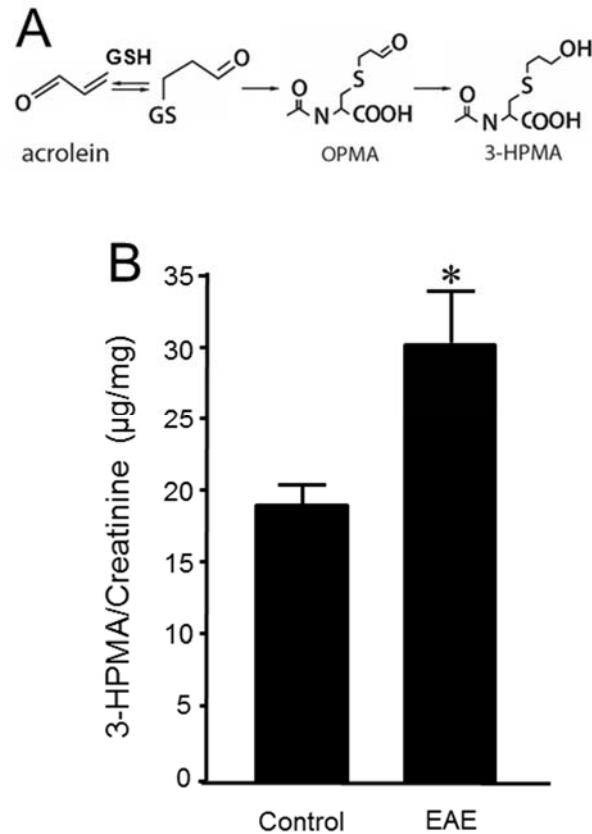


Figure 5.2 Determination of Acrolein Concentration Through Urine 3-HPMA Measurement in EAE Mice. (A). Chemical reaction of acrolein with glutathione (GSH) and production of subsequent metabolites OPMA and 3-HPMA. (B). Bar graph depicts the ratio of 3-HPMA and creatinine measured in urine of control and EAE mouse. Urine samples were collected approximately 21-23 days after MOG injection in EAE mouse when the behavior deficits peak. Each urine sample represents an accumulative volume of a 24 hr period. Age matched mice served as controls. Note the increase of 3-HPMA in urine in EAE. ($P < 0.05$ when compared to control, t-test). $N = 5$ in each group of 3-HPMA measurement in urine. Data expressed as average \pm SEM.

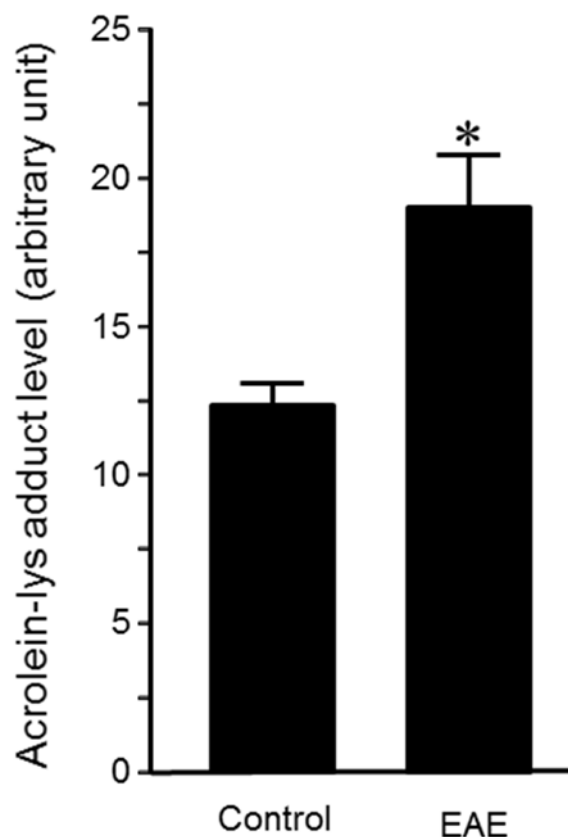


Figure 5.3 Elevations of CNS Acrolein Concentrations in EAE Mice. The acrolein-lysine adducts in control and in EAE were detected using Bio-Dot SF microfiltration apparatus. Band intensity were analyzed using image J (NIH) are expressed in arbitrary units. Note the Bar graph demonstrated the increase of acrolein-lysine adducts in EAE. ($P < 0.05$ when compared to control, t-test). $N = 4$ in each group of acrolein measurement in tissue.

5.3.2 Multiple Sclerosis Patients Exhibited Increased 3-HPMA in Urine and Serum

Urine and serum samples were collected from diagnosed MS patients (urine: $n=40$; serum: $n=41$) and volunteer controls consisting of mainly office staff and family members of patients (urine: $n=23$; serum $n=23$). Acrolein content within the specimens was reflected through the assessment of 3-HPMA using LC/MS/MS. Figure 5.4 depicts 3-HPMA measurements as both an mean value and

as a scatter plot to show distribution of urinary 3-HPMA levels within the group. Mean 3-HPMA levels detected in the urine of MS patients were significantly elevated relative to healthy controls. Furthermore, multiple patients exhibited urinary 3-HPMA levels that exceeded the maximum 3-HPMA level detected in the control group. Results obtained following quantification of 3-HPMA in patient serum specimens corresponded with the values obtained from urine analysis for both the MS group and the control group, in which MS patients demonstrated a significant elevation compared to control (Fig 5.5). The scatter plot also shows a similar distribution of the data in which a number of MS patients exceeded the maximum serum 3-HPMA value obtained from the control group. Interestingly, a correlation analysis between 3-HPMA measurements in MS patient urine and serum samples, revealed a significant positive relationship (Fig 5.6).

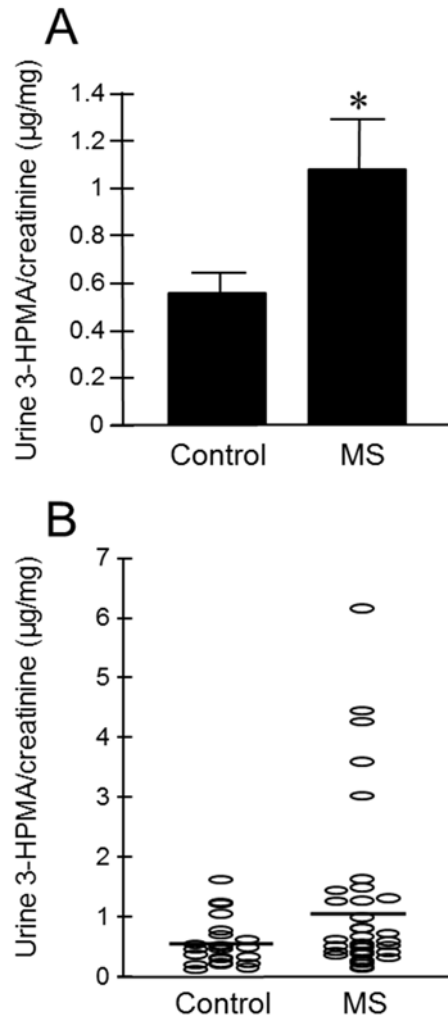


Figure 5.4 Determination of Acrolein Concentration Through Urine 3-HPMA Measurement in MS Patients and Healthy Individuals. The MS patient group including relapsing-remitting (RR), primary progressive (PP), and secondary progressive (SP) types of MS. (A). Bar graph demonstrate the average value of urine 3-HPMA. Specifically, the average concentration of 3-HPMA is 1.094 ± 0.212 µg/mg creatinine for MS patients (N = 40) and 0.570 ± 0.082 µg/mg creatinine for healthy individuals (N = 23). Note the increase of 3-HPMA in urine in MS patients. (*: $P < 0.05$ when compared to control, *t*-test). Data expressed as average \pm SEM. (B). A scatter plot of the same data used in (A), including all the data points to reveal the range and distribution of measured values. Solid lines indicate the average of 3-HPMA in both MS and healthy control individuals. Note that while many data points of MS patients were distributed in the same range as that of control, there were still multiple points of MS were greater than that in control, some by multiple folds

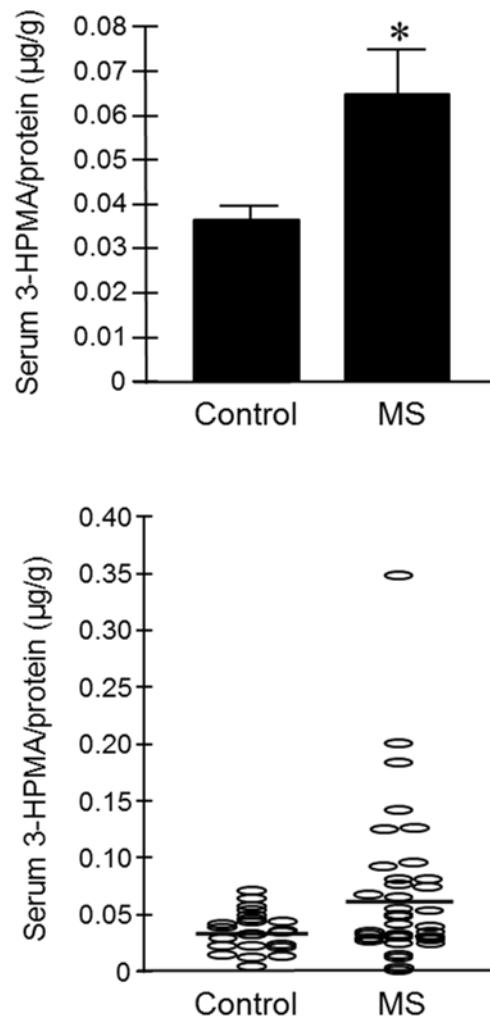


Figure 5.5 Determination of Acrolein Concentration Through Serum 3-HPMA Measurement in MS Patients and Healthy Individuals. The MS patient group including RR, PP, and SP types of MS. (A). Bar graph demonstrate the average value of serum 3-HPMA. Specifically, the average concentration of 3-HPMA is 0.065 ± 0.009 $\mu\text{g/g}$ protein for MS patients ($N = 41$) and 0.036 ± 0.004 $\mu\text{g/g}$ protein for healthy individuals ($N = 23$). Note the increase of 3-HPMA in serum among MS patients. (\square : $P < 0.01$ when compared to control, t-test). Data expressed as average \pm SEM. (B). A scatter plot of the same data used in (A), including all the data points to reveal the range and distribution of measured values. Solid lines indicate the average level of acrolein in both MS patients and control individuals. Note that while many data points of MS patients were distributed in the same range as that of control, there were still multiple points of MS were greater than that of control, some by multiple folds.

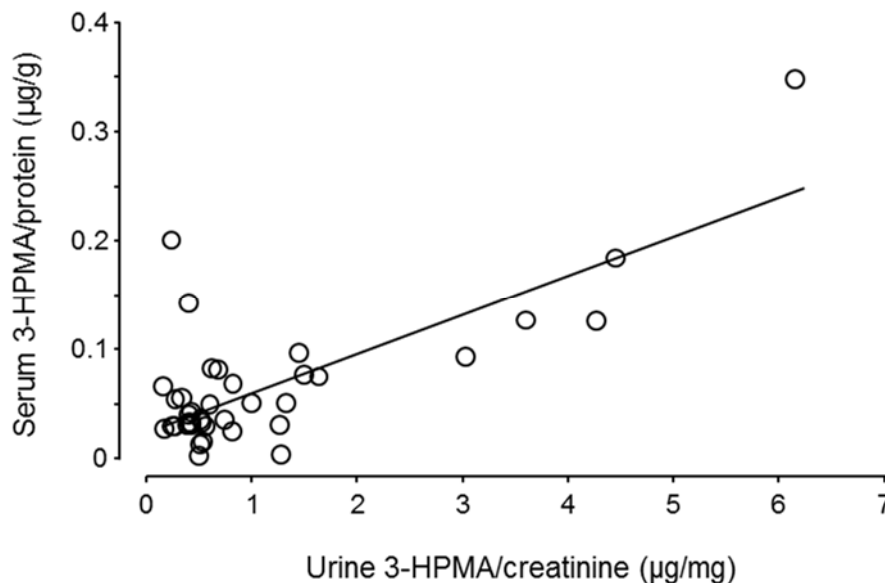


Figure 5.6 Correlation of 3-HPMA Levels in Urine and Serum in MS patients. The urine 3-HPMA is plotted against serum 3-HPMA for 39 MS patients showing the relation between these two parameters. Urine and serum were collected at the same time for all patients. As indicates, the increase of urine 3-HPMA seems to accompanied by the elevation of serum 3-HPMA. Statistical analysis of correlation revealed A Pearson correlation coefficient r -value of 0.75, ($p < 0.0001$, two tailed).

5.4 Concluding summary

The 3-HPMA detection method is a significant advancement in the field of acrolein research and allows investigators to quantify endogenous acrolein levels in clinical scenarios. Furthermore, since 3-HPMA is a specific adduct for acrolein and GSH, 3-HPMA elevations can only be attributed to an increase in endogenous acrolein concentration. Prior to the establishment of this method, endogenous acrolein research in the CNS was largely limited to animal studies due to the invasive nature of other acrolein quantification methods, which require a fresh tissue sample. In a prior study, we reported acrolein elevations in the spinal cord tissue of EAE mice and that the application of an acrolein-scavenger, hydralazine,

effectively reduced acrolein levels, delayed symptom onset and reduced severity of motor deficits (Leung 2011). However, to our knowledge, urine 3-HPMA quantification has not been previously employed in the EAE model to assess systemic acrolein levels.

In the current study, when EAE mice exhibited peak deficit (days 21-23), urine samples were collected from both EAE and control groups. At the study conclusion (day 28) mice were euthanized and spinal cords were harvested for assessment of acrolein-lysine adducts to verify the 3-HPMA method. Concordantly, EAE mice exhibited elevated 3-HPMA and acrolein levels relative to control mice. The success of non-invasive acrolein detection in urine permits longitudinal in vivo studies of acrolein dynamics, evaluation of anti-acrolein therapies and, most notably, detection of acrolein in human patients. As acrolein has already been established as a novel therapeutic target in EAE, the current study was primarily intended at investigating the pathological role of acrolein in clinical cases of MS.

The clinical component of this study exclusively relied on 3-HPMA quantification as an acrolein detection method, however 3-HPMA was independently quantified in both urine and serum samples to ensure the reliability of the measurements. In both urine and serum, mean 3-HPMA was significantly elevated in MS patients relative to controls indicating that acrolein may play a similar role in EAE and MS and the acrolein-scavenging in MS patients could potentially have therapeutic benefit. Interestingly, 3-HPMA concentration in urine was an order of magnitude greater than that detected in serum samples. This

discrepancy can potentially be attributed to a larger total volume of serum than urine and also that as acrolein is removed from circulation by the renal system, excreted waste is more concentrated.

Clinical detection of increased acrolein levels in MS not only implicates acrolein as a pathological target, but also prompts further investigation of the utility of acrolein as a biomarker for diagnosis, disease monitoring and guiding therapeutic regimens. As previously discussed, acrolein is primarily a clinical diagnosis supplemented by neuroimaging and other laboratory tests. However, the presence of MS symptoms accompanied by an elevated acrolein level may potentially allow a physician to establish an MS diagnosis in the future from a thorough history, physical exam and a collection of a urine sample. Additionally, acrolein may also have clinical applicability as a biomarker to predict relapses or clinical progression in later stages of the disease in which remission no longer occurs. To investigate acrolein as a potential biomarker for disease monitoring, additional clinical studies are needed to examine acrolein at multiple time points in the same patient, particularly shortly prior to and during relapses when MS is in an active stage.

If 3-HPMA elevations are observed prior to development of new symptoms, then there is potential for acrolein scavengers to be administered in an effort to decrease severity or latency of the relapse. Acrolein detection would also enable a more personalized approach to the treatment of MS. As can be observed in the scatter plots (Figure 5.4, 5.5), some MS patients exhibited 3-HPMA values that did not appear to be significantly elevated relative to controls. While it is possible that these patients were not exhibiting acrolein elevations due to remission, it raises

the plausibility that some MS patients may not benefit from anti-acrolein therapy. Non-invasive acrolein detection also allows for dosage of acrolein scavengers to be tailored to a specific patient. In summary, the noninvasive 3-HPMA detection method and availability of FDA-approved compounds capable of scavenging acrolein, hydralazine and phenelzine, underscores the translational nature of acrolein research which could potentially revolutionize current therapeutic approaches to the treatment and management of MS.

CHAPTER 6. RESPIRATORY EXPOSURE TO ACROLEIN

6.1 Introduction

Acrolein is exogenously present as a pollutant generated by the incomplete combustion of wood, petrol and plastic, industrial processes, smoking of tobacco products and frying of foods in oil [48]. Similarly to acrolein produced endogenously, environmental sources of acrolein have the potential to be systemically absorbed by the body and thus can react with biomolecules and inflict damage to virtually every organ system [103]. In fact, environmental acrolein exposure, particularly in the case of cigarette smoking, can elicit 3-HPMA elevations in urine that are two times greater than the level seen in non-smokers and upon cessation of smoking, 3-HPMA levels declined by approximately 78% [104]. The amount of acrolein generated by burning cigarettes is highly dependent on the glycerin content, which varies from brand to brand, however acrolein is estimated to be present in concentrations of 56-69 μg in one cigarette [105].

Detrimental effects of cigarette smoking are well characterized and vast, as tobacco use has been linked to many pathologies spanning all the major organ systems. In fact, clinical cohort studies have reported that exposure to cigarette smoke directly, indirectly, and even in early life seems to be exacerbating the development and progression of MS functional loss [7, 10, 106-109]. However, the

pathophysiological mechanisms underlying this relationship remain elusive and the individual compound(s) within cigarette smoke that are contributing have yet to be ascertained. In a previous study aimed at assessing the impact of tobacco use through both inhalation and oral routes, have found no apparent association between oral tobacco use and MS, indicating that nicotine does not play a role. Therefore a compound in tobacco, other than nicotine, that is present in greater concentrations upon burning appears to be the culprit [110]. Due to the established connection between MS and endogenous acrolein levels, the association between MS and exogenous acrolein exposure, specifically through inhalation when smoking or in close proximity to smokers, warrants further investigation.

6.1.1 Cigarette Smoking in Humans

As the single most preventable cause of death, cigarette smoke is a universally known environmental pollutant, producing a array of harmful chemicals that are detrimental to human health leading to various illnesses or death [111]. Exposure occurs through primary and secondary sources that few can avoid in our modern society given that one in five adults in the US are current cigarette smokers [21, 111]. Specifically relating to our interests, cigarette smoke is suspected of exacerbating multiple sclerosis and other neuropathologies as evidenced by recent clinical and laboratory observations [7, 10, 106-109]. This concern is further fueled by taking into consideration that patients with neurological disabilities tend to be more avid, heavier smokers, who are less likely to quit compared to general population [111].

Acrolein is endogenously elevated in animal models and clinical cases of MS and also is an emission component of tobacco smoke [56, 105]. It has been demonstrated that systemic and CNS acrolein levels increase following respiratory exposure to acrolein [104, 112]. Due to its neurotoxic nature, its commonality between MS and tobacco emissions, and epidemiological studies linking MS and cigarette smoking, it is possible that acrolein is capable of accumulating from environmental exposure and worsening clinical course for MS patients who smoke tobacco. In order to further study this relationship, an animal model for acrolein inhalation was established and preliminary animal studies were conducted to ascertain the relationship between respiratory acrolein exposure and accumulation both systemically and locally within the CNS.

6.1.2 Acrolein Inhalation in Mice

To further investigate the effect of respiratory acrolein exposure in the CNS, it is imperative to determine if inhalation of exogenous acrolein can affect endogenous systemic 3-HPMA levels detected by LC/MS/MS in a controlled animal study. The current study was performed to examine the hypothesis that acute respiratory exposure to acrolein can evoke an increase in endogenous acrolein levels. More specifically, since MS is a disease of the CNS, the ability of acrolein to accumulate in the brain and spinal cord following respiratory exposure could have serious implications in the understanding clinically reported links between cigarette smoking and MS. Following respiratory exposure to acrolein at a concentration relevant to that in cigarette smoke for three weeks, urinary 3-HPMA and acrolein-lysine adducts in the spinal cord were both increased relative

to the sham and control groups. This data is indicative that acrolein is capable of systemic absorption through the pulmonary circulation and, furthermore, can cross the blood brain barrier to infiltrate the CNS.

6.2 Materials and methods

6.2.1 Respiratory Exposure to exogenous acrolein

An air-tight chamber made of plexiglass (10 in. x 14 in. x 6 in.) was made in our laboratory and placed in a ventilation hood (Fig. 6.1). A compressed gas cylinder containing an acrolein air mixture of ~350ppm (Praxair, Geismar, LA, USA) was adjusted by delivering controlled volumes of ambient air from a compressed gas cylinder (Indiana Oxygen, IN, USA) using two flowmeters (Aalborg, Orangeburg, NY, USA). The diluted acrolein:air mixture was then forced into the chamber through an input valve. Exhaust from the chamber was expelled through an output valve and passed through an activated charcoal filter (VetEquip, Pleasanton, CA, USA) within the ventilation hood. Final delivered concentration in the current study was 1.5 ppm acrolein in air, a concentration verified using GC/MS. Gas samples from the chamber were obtained using a vacutainer (BD, Franklin Lakes, NJ, USA) and GC/MS analysis was carried out as outlined below.

Mice were divided into three groups: control, sham, and acrolein. The control group were not exposed to the inhalation chamber. Animals from the sham group were placed in the chamber and received a controlled volume of ambient air, while the acrolein group was exposed to 1.5 ppm acrolein in air. Exposure paradigm for the sham and acrolein mice was 30 minute sessions, twice a day, for an observation period of three weeks.

6.2.2 Gas chromatography/Mass Spectrometry

A Pegasus 4D gas chromatography/gas chromatography time-of-flight mass spectrometer (GCxGC/TOF-MS, LECO Corporation, St. Joseph, MI), with a CTC CombiPAL autosampler (LEAP Technologies, Carrboro, NC) was used for sample analysis. Prior to injection, samples (0.5 mL) were agitated for 5 minutes at 80°C and 500RPM. An Rtx-65 capillary column (Restek, 30 m x 0.25 mm x 0.25 um) and high purity helium (carrier gas, 1.0 ml/min, 10:1 split ratio) were selected. Temperature program was set to begin at 40°C (3 minute hold time) and then increased to 140°C at a rate of 20°C/min. Temperature for the injection inlet temperature and the mass spectrometer transfer line were set to 130°C and 200°C, respectively. The electron impact ion source was maintained at 200 °C and filament bias was -70 V. Mass spectra were obtained from 23 to 200 m/z at 30 spectra/sec. Acrolein standards ranging from 33 and 3300 ppm were prepared and mass peaks of 55 and 56 were used for acrolein quantification. Acrolein retention time was 107 sec.

6.2.3 Detection of Acrolein-lysine Adducts Dot Immublotting

See 5.2.3

6.2.4. 3-Hydroxypropl Mercapturic Acid (3-HPMA) Quantification

See 5.2.8

6.2.5 Subject Recuritment\

See 5.2.5

6.2.6. Clinical Urine Collection

See 5.2.6

6.3 Results

6.3.1 Urine 3-HPMA/Creatinine Levels Increased Following Acrolein Inhalation in Mice

Urine samples were obtained at 0 (before inhalation), 1, 2, and 3 weeks post inhalation to determine the ability of acrolein to accumulate systemically and locally following respiratory exposure. Using LC/MS/MS urinary 3-HPMA levels were measured and the current data suggests a direct relationship between urine 3-HPMA concentration and duration of acrolein exposure. In other words, 3-HPMA levels were observed to steadily increase over the three week observation period (Fig 6.1 C). A significant elevation was observed from baseline ($11.46 \pm .05 \mu\text{g}/\text{mg}$) in measurements taken at both week 2 ($14.43 \pm 0.84 \mu\text{g}/\text{mg}$, $p < 0.05$) and 3 ($17.82 \pm 0.33 \mu\text{g}/\text{mg}$, $p < 0.01$). A significant increase was also detected between week 1 ($12.41 \pm 1.85 \mu\text{g}/\text{mg}$, $p < 0.05$) and week 3. Mice from the sham group did not demonstrate significant changes in urine 3-HPMA for the duration of the study.

6.3.2 Respiratory Acrolein Exposure Increases Acrolein-Lysine in Mouse Spinal Cord Tissue

At the study conclusion, fresh spinal cords were harvested for quantification of acrolein-lysine adducts to assess acrolein accumulation in the CNS. A dot immunoblotting assay was conducted using the spinal cord samples from the three experimental groups: acrolein, sham, and control (Fig 6.1 D). Acrolein-lysine adduct level in the spinal cords of mice following acrolein respiratory exposure for three weeks ($10.56 \pm 0.59 \text{ a.u.}$) was significantly increased compared to the sham group ($3.71 \pm 0.58 \text{ a.u.}$, $p < 0.05$), or control group ($4.52 \pm 1.97 \text{ a.u.}$, $p < 0.05$).

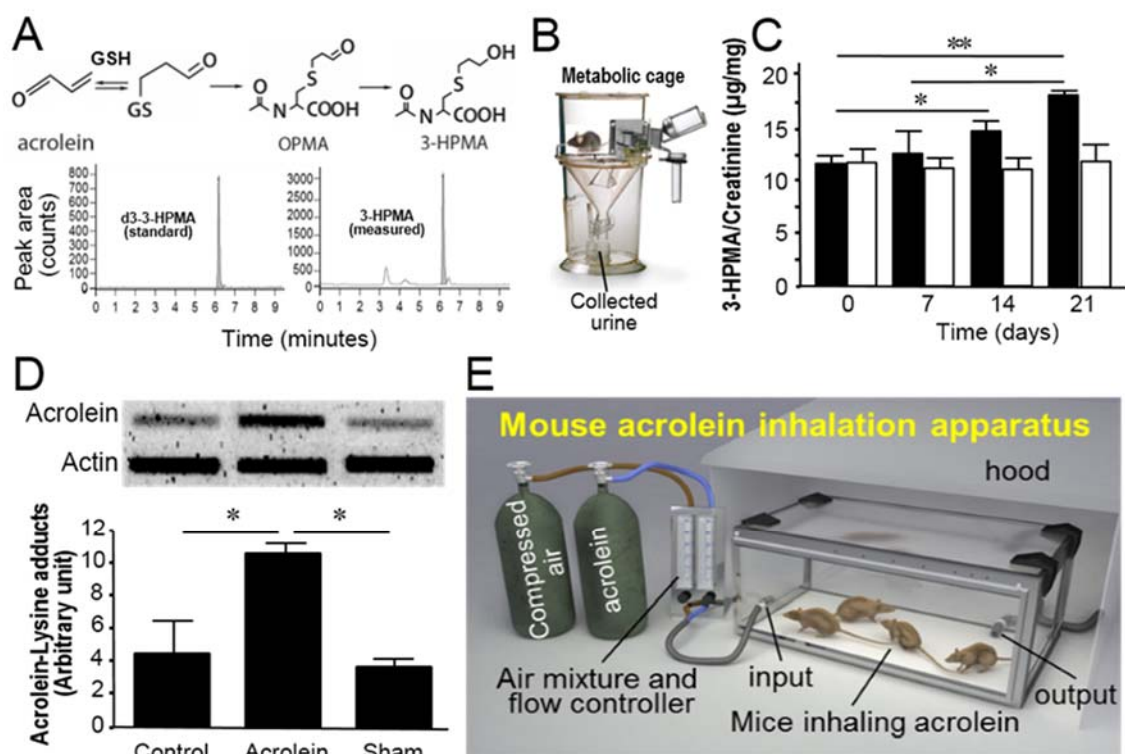


Figure 6.1 Preclinical Assessment of the Effects of Respiratory Acrolein Exposure in Mice. (A) Acrolein reaction with glutathione and production of subsequent metabolites OPMA and 3-HPMA. Bottom: Mass spectra outputs of d3-3-HPMA (Standard) and 3-HPMA measurements obtained from mouse urine. (B) Metabolic cage used for urine collection. (C) Bar graph displaying the ratio of 3-HPMA and creatinine measured in urine of acrolein-inhaled mouse at day 0 (11.46 ± 0.50), day 7 (12.41 ± 1.85), day 14 (14.43 ± 0.84), and day 21 (17.82 ± 0.33) of acrolein exposure (acrolein group: Filled bars). 3-HPMA concentrations for the sham group were at day 0 (11.80 ± 1.57), day 7 (11.29 ± 1.17), day 14 (11.09 ± 1.34), and day 21 (12.02 ± 2.02) (sham group: open bars). ANOVA comparisons among acrolein group yielded $p < 0.05$ between days 0 and 14, and days 7 and 21; $p < 0.01$ between days 0 and 21. No significance were found within sham group. Values are expressed as mean \pm SEM. $N = 5-10$ in all conditions. (D) Dot immunoblotting results comparing levels of acrolein-lysine adducts in the spinal cord tissue of animals from each of the three groups. Bar graph displays that the acrolein-lysine levels in acrolein group (10.56 ± 0.59 a.u.) is significantly higher than those in sham group (3.71 ± 0.58 a.u.), and control group (4.52 ± 1.97 a.u.) ($n=4$ in all groups, $\pm P < 0.05$, ANOVA). Values are expressed mean \pm SEM. (E) Diagram of inhalation setup.

6.3.3 Systematic 3-HPMA Elevation in MS Patients Who Are Self-Reported Cigarette Smokers

MS patients who identified as tobacco smokers, exhibited drastically increased 3-HPMA levels (7.1 ± 2.9 ; $n=6$) relative to non-smoker MS patients (1.094 ± 0.212 ; $n=40$; $P < 0.05$) (Fig 6.2). Furthermore, MS smokers exhibited significantly elevated EDSS scores (4.25 ± 1.03 ; $n=6$) compared to MS nonsmokers (1.55 ± 0.39 ; $n=40$; $P < 0.05$) (Figure 6.3). We hypothesize that the drastic increase is the result of an additive effect of respiratory exposure to acrolein, as a result of tobacco smoking, combined with pathologically elevated levels of acrolein resulting from oxidative stress. These clinical findings support data obtained in preclinical studies and provide further evidence that acrolein research is translational and data currently being obtained using the EAE model has high potential to be clinically applicable in MS patients.

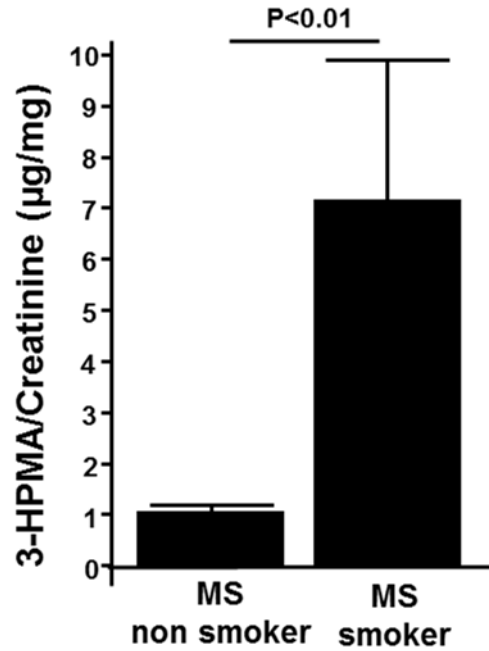


Figure 6.2 Smoking in MS Patients is Associated with Higher Urine 3-HPMA

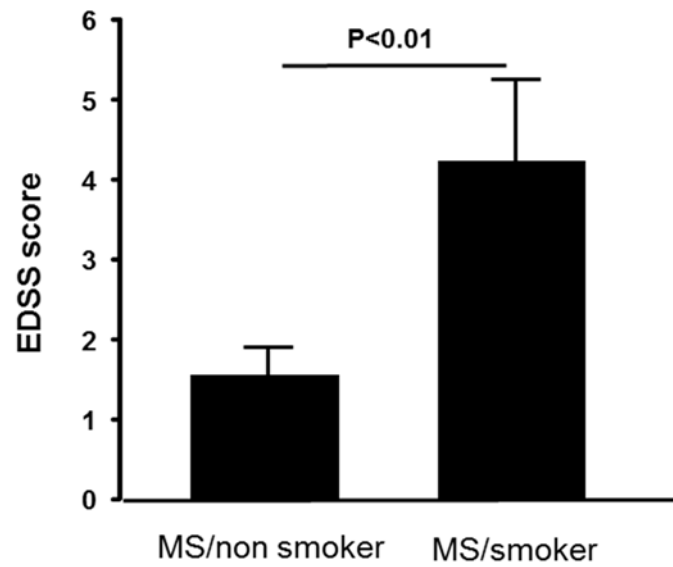


Figure 6.3 Smoking Cigarettes is Associated with Higher EDSS Scores in Multiple Sclerosis Patients.

6.4 Discussion

The current study concludes that exposure to acrolein in the respiratory system results in systemic absorption of acrolein and infiltration of acrolein into the CNS across the blood brain barrier. Specifically, an increase in the acrolein-GSH metabolite, 3-HPMA, can be elicited in a controlled animal model following acrolein respiratory exposure at a concentration relevant to that in cigarette smoke. Furthermore, local concentrations of acrolein in the CNS were found to be elevated in mice as indicated by acrolein-lysine adduct levels within the spinal cords of animals that inhaled acrolein. These findings are consistent with previous clinical observations, which reported that human cigarette smokers exhibited higher levels of urine 3-HPMA by 5-10 times when compared to nonsmokers [104, 113]. However, subject smoking histories were significantly longer than the three week period modeled in this study, with most patients reporting regular cigarette consumption over a period of years. Due to the constraints of clinical studies, primarily limited to retrospective cohort investigations, an adequate quantification study correlating aerosolized acrolein dosage and urine 3-HPMA level has not been conducted. The main advantage in the current study is the use of an animal model permits control of experimental conditions, such as the concentration, duration and paradigm of acrolein exposure.

Acrolein was shown to be effectively absorbed upon inhalation for no more than two weeks and aggregated in the blood stream, increasing 3-HPMA levels by 30% after two weeks and 60% after three weeks of exposure (Fig 6.1 C).

An acrolein concentration of 1.5 ppm was selected for the current study because of its use in previous animal studies, it is significantly lower than reported acrolein concentration in tobacco smoke and is well above the concentration of acrolein in ambient air, which may render it applicable in future studies examining acrolein accumulation following second-hand tobacco smoke exposure [114-121]. The exposure paradigm of two 30 minute exposures per day was employed in an attempt to mimic smoking a half a pack or 12 cigarettes per day. This rough calculation was based on the assumption that a cigarette burns for 5 minutes and the total daily 60 minute exposure time was adjusted to be two 30 minute exposures to allow animals to recover following acrolein inhalation and minimize acute toxicity. In a 2010 report, the CDC estimated that the average American tobacco user smokes 20 cigarettes daily indicating that if this estimation is correct, mice were exposed to less acrolein daily than the average smoker.

Increase in 3-HPMA level following respiratory acrolein exposure in mice was an expected outcome in this study, as it has been previously demonstrated clinically [104, 113]. However, the ability of acrolein to accumulate locally in the CNS following acute acrolein inhalation was of particular interest given the role of acrolein in cases of neurological disease and trauma [44, 58, 95, 98, 100]. The increased presence of acrolein-lysine adducts in the spinal cords of mice subjected to acrolein inhalation suggests that acrolein is not confined to systemic circulation upon absorption through the lungs, but rather is able to disperse into the CNS and likely other tissues. Previous data indicating the pathological role of endogenously produced acrolein in EAE and MS, raises the hypothesis that environmental

exposure to acrolein could impact clinical course, potentially exacerbating symptoms or accelerating disease pathogenesis and progression[56].

Known relationships between both acrolein and cigarette smoking, acrolein and clinical MS and animal models, and clinical observations of adverse effects of smoking in MS patients suggest that the relationship between acrolein, smoking and MS warrants further study. This is further supported by data from this study, indicating that 3-HPMA is significantly higher in MS patients who self-reported as cigarette smokers compared to MS patients who did not smoke. Furthermore, MS smokers demonstrated significantly higher EDSS scores at the time of sample collection, indicating that higher 3-HPMA levels could potentially correspond with a more severe clinical course. Given the data indicating that endogenous acrolein levels are elevated in MS patients and the successful application of acrolein scavengers in EAE mice, clinical application of acrolein scavengers may serve as a potential therapeutic approach in MS, especially in MS patients who smoke cigarettes.

CHAPTER 7. ACROLEIN ELEVATION IN BOTH RR MS PATIENTS AND RR EAE AND SYMPTOM ALLEVIATION IN RR EAE BY HYDRALAZINE

7.1 Introduction

RR MS is the most common subtype of MS, representing nearly 85% of current MS cases [13]. However, to date, research of acrolein in MS animal models has exclusively been conducted in EAE mice induced with a MOG emulsion, which mimics the PP and SP disease subtypes. In order to facilitate the translation of acrolein research to the therapeutic tools in the MS patient population, it is crucial to investigate the clinically observed acrolein elevations in RR MS patients, by conducting an investigation similar to that conducted by Leung and colleagues in 2011 in an animal model that mimics RR MS disease course. In the current study, a PLP emulsion was used to induce RR EAE in mice [56]. Analyses of urine samples and CNS tissue samples are ongoing, however materials and methods, preliminary findings and a brief discussion are presented in the following sections.

7.2 Materials and methods

7.2.1 Subject Enrollment

See 5.2.5

7.2.2 Clinical Urine Collection

See 5.2.6

7.2.3 Clinical Serum Collection

See 5.2.7

7.2.4 RR EAE induction and behavioral assessment

Female SJL mice were injected with 0.5 mL PLP/Complete Freund's adjuvant emulsion at a total of four sites; two subcutaneously bilaterally to the caudal spinal column (shoulders) and two subcutaneously bilaterally to the rostral ends of the spinal column (hips) (Hooke Laboratories, Lawrence, MA). The emulsion triggers autoimmune recognition of PLP by T-cells and due to nature of immune response most closely mimics clinical MS. Behavioral assessment was carried out in accordance with the scale provided by Hooke, briefly described below. 0—no deficit; 0.5—limp tip of tail; 1.0—complete tail paralysis; 1.5—limp tail + hindlimb inhibition; 2.0—limp tail + hindlimb weakness; 2.5—limp tail + hindlimb dragging; 3.0—limp tail + complete hindlimb paralysis; 3.5—3.0 score + hunched appearance or inability to rollover if placed on its side; 4.0—3.0 score + partial forelimb paralysis; 4.5—4.0 score + lethargy and minimal responsiveness to sensory stimulation; 5.0—mouse rolling around cage or death/euthanization.

7.2.5 Hydralazine Preparation and Application

Hydralazine hydrochloride was prepared for a final delivery concentration of 1 mg/kg following dissolution in phosphate buffered saline. The solution was then filtered for sterilization. Beginning from the day of model induction, mice received daily intraperitoneal injections of hydralazine until study conclusion 45 days post-induction.

7.2.6 Animal Urine Collection

See 5.2.4

7.2.7 3-HPMA Analysis *In Progress*

See 5.2.8

7.2.8 Dot Immunoblotting *In progress*

See 5.2.3

7.3 Preliminary Results

7.3.1 Clinical 3-HPMA Elevations in Urine and Serum of RR MS Patients

A metabolite specific for acrolein following reaction with GSH, 3-HPMA, was detected at higher concentrations in the urine and serum of RR MS patients (urine: 1.123 ± 0.255 $\mu\text{g}/\text{mg}$ creatinine; serum: is 0.069 ± 0.013 $\mu\text{g}/\text{g}$ protein; $n=31$) relative to healthy controls (urine 0.570 ± 0.082 $\mu\text{g}/\text{mg}$ creatinine; serum: and 0.036 ± 0.004 $\mu\text{g}/\text{g}$ protein; $p < 0.05$ and $p < 0.01$, respectively; $n=23$) (Figure 7.1). Notably, while many data points of MS patients were distributed in the same range as that of control, there were still multiple points of MS that were greater than that of control, some by multiple folds.

7.3.2 Daily Hydralazine Application Ameliorated Motor Deficit in RR EAE Mice

Though 3-HPMA quantification and acrolein-lysine adduct assessment in spinal cords is not yet completed for this study, preliminary behavioral data suggests that acrolein is indeed elevated in RR EAE due to alleviation of motor deficit following hydralazine treatment. Furthermore, hydralazine seems to have effectively shortened relapse latency, delayed onset of symptoms and decreased severity during relapse, although statistical analyses of the data are also ongoing.

Furthermore, a number of MS patients who participated in the study, were found to have systemic 3-HPMA concentrations within the range of what is considered “normal”. The reason for the observed discrepancy could lie in the relapsing-remitting nature of the pathology. In other words, MS patients that exhibited nonpathological concentrations of acrolein could be in remission and not experiencing any symptoms. Longitudinal studies are warranted to pursue this line of investigation, to monitor acrolein dynamics in multiple phases of the disease, especially acrolein levels immediately preceding and during a relapse. In the event that an MS attack is able to be predicted by a rise in systemic acrolein concentration, this finding would revolutionize current therapeutic approaches to the diagnosis, symptom management and treatment regimens in the 2.5 million MS patients.

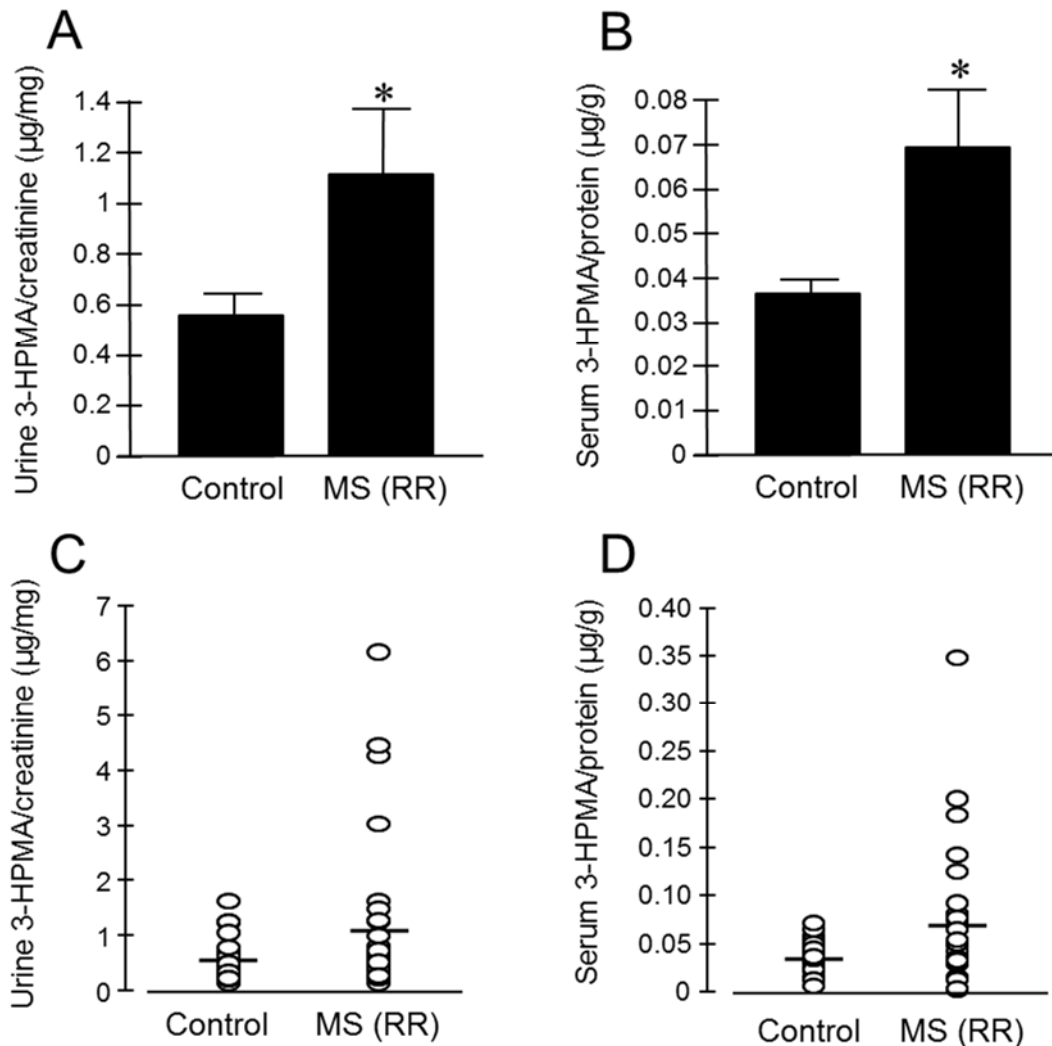


Figure 7.1 Quantification of 3-HPMA in the Urine and Serum of RR MS patients. (A). Bar graph demonstrate the average value of urine 3-HPMA. Specifically, the average concentration of urine 3-HPMA is 1.123 ± 0.255 µg/mg creatinine for RRMS patients (N = 31) and 0.570 ± 0.082 µg/mg creatinine for healthy individuals (N = 23). (*: P < 0.05 when RRMS were compared to control, *t*-test). (B) Bar graph demonstrate the average value of serum 3-HPMA. Specifically, the average concentration of serum 3-HPMA is 0.069 ± 0.013 µg/g protein for MS patients (N = 41) and 0.036 ± 0.004 µg/g protein for healthy individuals (N = 23). (*: P < 0.01 when RRMS were compared to control, *t*-test). Data in A and B is expressed as average \pm SEM. (C) and (D). Scatter plot of the same data used in (A) and (B), including all the data points to reveal the range and distribution of measured values. Solid lines indicate the average level of 3-HPMA in both MS patients and control individuals in urine (C) and in serum (D).

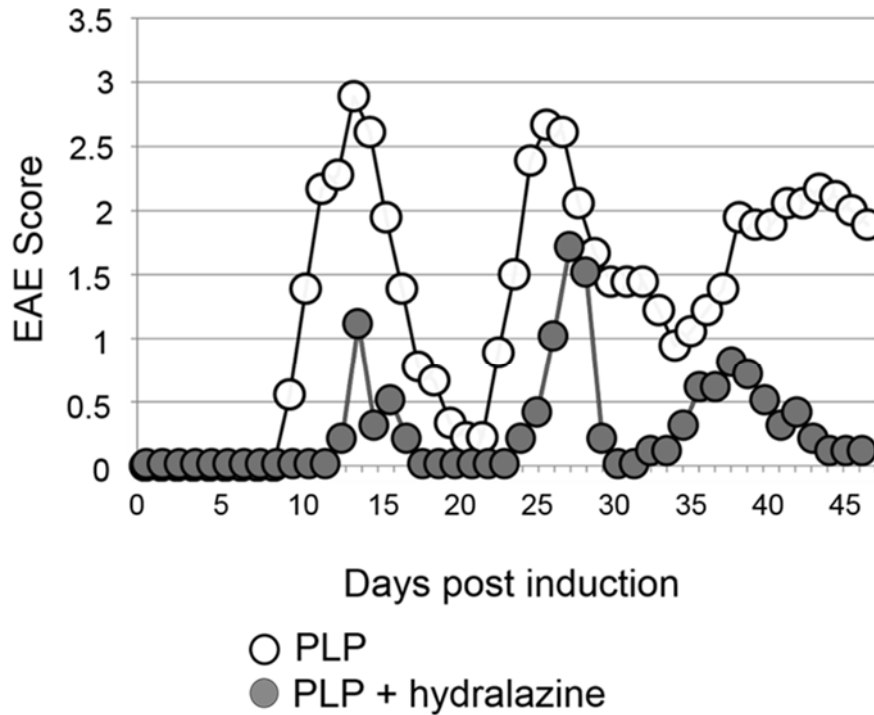


Figure 7.2 Hydralazine Application in RR EAE Alleviates Motor Deficit.

7.4 Discussion of Preliminary Findings

In order to determine the clinical applicability of acrolein research it is important to investigate its pathological role in each subtype of MS. To our knowledge, the current study is the first to focus on detecting and pharmacologically targeting acrolein in an RR EAE model, induced using a PLP/Complete Freund's adjuvant emulsion. Although, analyses of data obtained from this study is ongoing, clinical acrolein assessment in RR MS patients and observed behavioral trends in RR EAE with and without the application of acrolein scavenger hydralazine. Our findings strongly suggest that acrolein underlies symptomatic development in RR EAE, indicated by therapeutic benefit of acrolein

removal and in RR MS indicated by the concordant increase of acrolein in MS patient urine and serum samples compared to healthy controls.

In light of this evidence, we hypothesize that the 3-HPMA and dot immunoblotting analyses scheduled to be performed in this study, will indicate both a local and systemic rise in acrolein and that anti-acrolein therapy is neuroprotective, preserving CNS structure and alleviating pathological acrolein concentrations contributing to symptomatic development in MS patients.

CHAPTER 8. FUTURE DIRECTIONS

8.1 Examine the Effects of Exogenous Acrolein Exposure on Development of the EAE Model

Current data indicates that acrolein is potentially an underlying pathological factor linking MS and tobacco smoking and could explain the observation in epidemiological studies and in clinical data presented above indicating that cigarette consumption exacerbates MS symptoms and may accelerate disease progression. In order to further explore the relationship between acrolein, MS and cigarette smoking, a comprehensive study must be carried out in an EAE model, in which animals are subjected to respiratory acrolein exposure in controlled experimental setting. We propose a study consisting of three experimental groups: EAE mice exposed to respiratory acrolein with sham saline treatment, EAE mice exposed to respiratory acrolein with hydralazine treatment and EAE mice with sham acrolein inhalation exposure and sham saline treatment. If exposure to respiratory acrolein is capable of exacerbating symptoms and/or accelerating disease onset/progression in the EAE model, this would indicate acrolein is at least partially responsible for symptoms in EAE. Alleviation of these affects and attenuation of motor deficits following the application of an acrolein scavenger in EAE mice subjected to acrolein inhalation would provide further evidence of the validity and the translational nature of this relationship. Furthermore, if the results

from the animal model are consistent with observations in clinical MS cases, avoidance of exogenous acrolein exposure in cigarettes, fried food, pollution and occupational settings could prove to be a useful preventative care strategy to establish public health guidelines for people at risk for developing MS..

8.2 Employment of Minimally Invasive Neuroimaging Techniques with 3-HPMA Quatification to Determine How Endogenous Acrolein Concentration Corresponds with CNS Structural Damage

In order to establish acrolein as a biomarker in EAE and MS, a study that quantifies both degree of CNS structural disruption and endogenous acrolein concentration is warranted. Such a study would reveal if there is a positive relationship between acrolein levels and disease activity and if, more importantly, if increases in acrolein values could potentially be used to predict relapses in both the RR EAE model or clinical MS cases. The clinical applicability and noninvasive nature of the 3-HPMA detection in combination with MRI (structural and Gd-contrast) imaging, ensures the feasibility of this line of questioning in both a controlled EAE model and MS patients. Knowledge gained from this line of questioning has the potential to revolutionize clinical approaches for diagnosis, guiding therapeutic regimens and monitoring disease activity in MS patients..

REFERENCES

REFERENCES

1. Alonso, A. and M.A. Hernan, Temporal trends in the incidence of multiple sclerosis: a systematic review. *Neurology*, 2008. 71(2): p. 129-35.
2. Trapp, B.D. and K.A. Nave, Multiple sclerosis: an immune or neurodegenerative disorder? *Annu Rev Neurosci*, 2008. 31: p. 247-69.
3. Koch-Henriksen, N. and P.S. Sorensen, The changing demographic pattern of multiple sclerosis epidemiology. *Lancet Neurol*, 2010. 9(5): p. 520-32.
4. Hirst, C., et al., Survival and cause of death in multiple sclerosis: a prospective population-based study. *J Neurol Neurosurg Psychiatry*, 2008. 79(9): p. 1016-21.
5. Kobelt, G., et al., Costs and quality of life in multiple sclerosis: a cross-sectional study in the United States. *Neurology*, 2006. 66(11): p. 1696-702.
6. Gupta, G., J.M. Gelfand, and J.D. Lewis, Increased risk for demyelinating diseases in patients with inflammatory bowel disease. *Gastroenterology*, 2005. 129(3): p. 819-26.
7. Heinzlef, O., et al., Autoimmune diseases in families of French patients with multiple sclerosis. *Acta Neurol Scand*, 2000. 101(1): p. 36-40.
8. Karni, A. and O. Abramsky, Association of MS with thyroid disorders. *Neurology*, 1999. 53(4): p. 883-5.
9. Nielsen, N.M., et al., Type 1 diabetes and multiple sclerosis: A Danish population-based cohort study. *Arch Neurol*, 2006. 63(7): p. 1001-4.
10. Compston, A. and A. Coles, Multiple sclerosis. *Lancet*, 2002. 359(9313): p. 1221-31.
11. Paty, D., et al., MS COSTAR: a computerized patient record adapted for clinical research purposes. *Ann Neurol*, 1994. 36 Suppl: p. S134-5.
12. Lublin, F. and A. Miller, Multiple sclerosis and other demyelinating disorders of the central nervous system, in *Neurology in Clinical Practice*, W.G. Bradley, R.B. Daroff, and G.M. Jankovic, Editors. 2008, Butterworth-Heinemann: Philadelphia. p. 1584-8.

13. Compston, A. and A. Coles, Multiple sclerosis. *Lancet*, 2008. 372(9648): p. 1502-17.
14. Miller, D.H. and S.M. Leary, Primary-progressive multiple sclerosis. *Lancet Neurol*, 2007. 6(10): p. 903-12.
15. McDonald, W.I., et al., Recommended diagnostic criteria for multiple sclerosis: guidelines from the International Panel on the diagnosis of multiple sclerosis. *Ann Neurol*, 2001. 50(1): p. 121-7.
16. Montalban, X., et al., MRI criteria for MS in patients with clinically isolated syndromes. *Neurology*, 2010. 74(5): p. 427-34.
17. Polman, C.H., et al., Diagnostic criteria for multiple sclerosis: 2005 revisions to the "McDonald Criteria". *Ann Neurol*, 2005. 58(6): p. 840-6.
18. Rovira, A., et al., A single, early magnetic resonance imaging study in the diagnosis of multiple sclerosis. *Arch Neurol*, 2009. 66(5): p. 587-92.
19. Swanton, J.K., et al., MRI criteria for multiple sclerosis in patients presenting with clinically isolated syndromes: a multicentre retrospective study. *Lancet Neurol*, 2007. 6(8): p. 677-86.
20. Polman, C.H., et al., Diagnostic criteria for multiple sclerosis: 2010 revisions to the McDonald criteria. *Ann Neurol*, 2011. 69(2): p. 292-302.
21. Frischer, J.M., et al., The relation between inflammation and neurodegeneration in multiple sclerosis brains. *Brain*, 2009. 132(Pt 5): p. 1175-89.
22. Roach, E.S., Is multiple sclerosis an autoimmune disorder? *Arch Neurol*, 2004. 61(10): p. 1615-6.
23. Weiner, H.L., Multiple sclerosis is an inflammatory T-cell-mediated autoimmune disease. *Arch Neurol*, 2004. 61(10): p. 1613-1615.
24. Lucchinetti, C., et al., Heterogeneity of multiple sclerosis lesions: implications for the pathogenesis of demyelination. *Ann Neurol*, 2000. 47(6): p. 707-17.
25. Oksenberg, J.R., et al., Selection for T-cell receptor V beta-D beta-J beta gene rearrangements with specificity for a myelin basic protein peptide in brain lesions of multiple sclerosis. *Nature*, 1993. 362(6415): p. 68-70.

26. Zhang, J., et al., Increased frequency of interleukin 2-responsive T cells specific for myelin basic protein and proteolipid protein in peripheral blood and cerebrospinal fluid of patients with multiple sclerosis. *J Exp Med*, 1994. 179(3): p. 973-84.
27. Block, M.L. and J.S. Hong, Microglia and inflammation-mediated neurodegeneration: multiple triggers with a common mechanism. *Prog Neurobiol*, 2005. 76(2): p. 77-98.
28. Hohlfeld, R., Biotechnological agents for the immunotherapy of multiple sclerosis. Principles, problems and perspectives. *Brain*, 1997. 120 (Pt 5): p. 865-916.
29. Bitsch, A., et al., Acute axonal injury in multiple sclerosis. Correlation with demyelination and inflammation. *Brain*, 2000. 123 (Pt 6): p. 1174-83.
30. Frohman, E.M., M.K. Racke, and C.S. Raine, Multiple sclerosis--the plaque and its pathogenesis. *N Engl J Med*, 2006. 354(9): p. 942-55.
31. Kornek, B., et al., Multiple sclerosis and chronic autoimmune encephalomyelitis: a comparative quantitative study of axonal injury in active, inactive, and remyelinated lesions. *Am J Pathol*, 2000. 157(1): p. 267-76.
32. Trapp, B.D., et al., Axonal transection in the lesions of multiple sclerosis. *N Engl J Med*, 1998. 338(5): p. 278-85.
33. Gold, R., C. Linington, and H. Lassmann, Understanding pathogenesis and therapy of multiple sclerosis via animal models: 70 years of merits and culprits in experimental autoimmune encephalomyelitis research. *Brain*, 2006. 129(Pt 8): p. 1953-71.
34. Coyle, J.T. and P. Puttfarcken, Oxidative stress, glutamate, and neurodegenerative disorders. *Science*, 1993. 262(5134): p. 689-95.
35. Hall, E.D., Free radicals and CNS injury. *Crit Care Clin*, 1989. 5(4): p. 793-805.
36. Hall, E.D. and J.M. Braugher, Free radicals in CNS injury. *Res Publ Assoc Res Nerv Ment Dis*, 1993. 71: p. 81-105.
37. Halliwell, B. and J.M.C. Gutteridge, Free radicals in biology and medicine. 3rd ed. Oxford science publications. 1999, Oxford, New York: Clarendon Press ;Oxford University Press. xxxi, 936 p.

38. Gilgun-Sherki, Y., E. Melamed, and D. Offen, The role of oxidative stress in the pathogenesis of multiple sclerosis: the need for effective antioxidant therapy. *J Neurol*, 2004. 251(3): p. 261-8.
39. Hall, E.D., Lipid peroxidation. *Adv Neurol*, 1996. 71: p. 247-57; discussion 257-8.
40. Bragt, P.C. and I.L. Bonta, Oxidant stress during inflammation: anti-inflammatory effects of antioxidants. *Agents Actions*, 1980. 10(6): p. 536-9.
41. Luo, J. and R. Shi, Acrolein induces axolemmal disruption, oxidative stress, and mitochondrial impairment in spinal cord tissue. *Neurochem Int*, 2004. 44(7): p. 475-86.
42. Smith, K.J., R. Kapoor, and P.A. Felts, Demyelination: the role of reactive oxygen and nitrogen species. *Brain Pathol*, 1999. 9(1): p. 69-92.
43. Bai, L., et al., Attenuation of mouse somatic and emotional inflammatory pain by hydralazine through scavenging acrolein and inhibiting neuronal activation. *Pain Physician*, 2012. 15(4): p. 311-26.
44. Hamann, K., et al., Critical role of acrolein in secondary injury following ex vivo spinal cord trauma. *J Neurochem*, 2008. 107(3): p. 712-21.
45. Logan, M.P., S. Parker, and R. Shi, Glutathione and ascorbic acid enhance recovery of Guinea pig spinal cord white matter following ischemia and acrolein exposure. *Pathobiology*, 2005. 72(4): p. 171-8.
46. Luo, J. and R. Shi, Diffusive oxidative stress following acute spinal cord injury in guinea pigs and its inhibition by polyethylene glycol. *Neurosci Lett*, 2004. 359(3): p. 167-70.
47. Moretto, N., et al., Acrolein effects in pulmonary cells: relevance to chronic obstructive pulmonary disease. *Ann N Y Acad Sci*, 2012. 1259(1): p. 39-46.
48. Esterbauer, H., R.J. Schaur, and H. Zollner, Chemistry and biochemistry of 4-hydroxynonenal, malonaldehyde and related aldehydes. *Free Radic Biol Med*, 1991. 11(1): p. 81-128.
49. Kehrer, J.P. and S.S. Biswal, The molecular effects of acrolein. *Toxicol Sci*, 2000. 57(1): p. 6-15.
50. Lovell, M.A., C. Xie, and W.R. Markesbery, Acrolein, a product of lipid peroxidation, inhibits glucose and glutamate uptake in primary cultures. *Free Radic Biol Med*, 2000. 29: p. 714-720.

51. Burcham, P.C., et al., Protein adduct-trapping by hydrazinophthalazine drugs: mechanisms of cytoprotection against acrolein-mediated toxicity. *Mol Pharmacol*, 2004. 65(3): p. 655-64.
52. Feng, Z., et al., Acrolein is a major cigarette-related lung cancer agent: Preferential binding at p53 mutational hotspots and inhibition of DNA repair. *Proc Natl Acad Sci U S A*, 2006. 103(42): p. 15404-9.
53. Ghilarducci, D.P. and R.S. Tjeerdema, Fate and effects of acrolein. *Rev Environ Contam Toxicol*, 1995. 144: p. 95-146.
54. Ho, S.S., et al., Carbonyl emissions from commercial cooking sources in Hong Kong. *J Air Waste Manag Assoc*, 2006. 56(8): p. 1091-8.
55. Magnusson, R., C. Nilsson, and B. Andersson, Emissions of aldehydes and ketones from a two-stroke engine using ethanol and ethanol-blended gasoline as fuel. *Environ Sci Technol*, 2002. 36(8): p. 1656-64.
56. Leung, G., et al., Anti-acrolein treatment improves behavioral outcome and alleviates myelin damage in experimental autoimmune encephalomyelitis mouse. *Neuroscience*, 2011. 173: p. 150-5.
57. Jensen, J.M. and R. Shi, Effects of 4-aminopyridine on stretched mammalian spinal cord: the role of potassium channels in axonal conduction. *J Neurophysiol*, 2003. 90(4): p. 2334-40.
58. Shi, Y., et al., Acrolein induces myelin damage in mammalian spinal cord. *J Neurochem*, 2011. 117(3): p. 554-64.
59. Sun, W., et al., Novel potassium channel blocker, 4-AP-3-MeOH, inhibits fast potassium channels and restores axonal conduction in injured guinea pig spinal cord white matter. *J Neurophysiol*, 2011. 103(1): p. 469-78.
60. Poliak, S. and E. Peles, The local differentiation of myelinated axons at nodes of Ranvier. *Nat Rev Neurosci*, 2003. 4(12): p. 968-80.
61. Blight, A.R., Effect of 4-aminopyridine on axonal conduction-block in chronic spinal cord injury. *Brain Res Bull*, 1989. 22(1): p. 47-52.
62. Shi, R. and A.R. Blight, Differential effects of low and high concentrations of 4-aminopyridine on axonal conduction in normal and injured spinal cord. *Neuroscience*, 1997. 77(2): p. 553-62.
63. Waxman, S.G., Demyelination in spinal cord injury and multiple sclerosis: what can we do to enhance functional recovery? *J Neurotrauma*, 1992. 9 Suppl 1: p. S105-17.

64. Waxman, S.G., D.A. Utzschneider, and J.D. Kocsis, Enhancement of action potential conduction following demyelination: experimental approaches to restoration of function in multiple sclerosis and spinal cord injury. *Prog Brain Res*, 1994. 100: p. 233-43.
65. Trapp, B.D., R. Ransohoff, and R. Rudick, Axonal pathology in multiple sclerosis: relationship to neurologic disability. *Curr Opin Neurol*, 1999. 12(3): p. 295-302.
66. Trapp, B.D. and P.K. Stys, Virtual hypoxia and chronic necrosis of demyelinated axons in multiple sclerosis. *Lancet Neurol*, 2009. 8(3): p. 280-91.
67. Hamann, K., et al., Hydralazine inhibits compression and acrolein-mediated injuries in ex vivo spinal cord. *J Neurochem*, 2008. 104(3): p. 708-18.
68. Shi, R., J. Luo, and M. Peasley, Acrolein inflicts axonal membrane disruption and conduction loss in isolated guinea-pig spinal cord. *Neuroscience*, 2002. 115(2): p. 337-40.
69. Cadenas, E. and K.J. Davies, Mitochondrial free radical generation, oxidative stress, and aging. *Free Radic Biol Med*, 2000. 29(3-4): p. 222-30.
70. Lenaz, G., et al., Role of mitochondria in oxidative stress and aging. *Ann N Y Acad Sci*, 2002. 959: p. 199-213.
71. Luo, J. and R. Shi, Acrolein induces oxidative stress in brain mitochondria. *Neurochem Int*, 2005. 46(3): p. 243-52.
72. Picklo, M.J. and T.J. Montine, Acrolein inhibits respiration in isolated brain mitochondria. *Biochim Biophys Acta*, 2001. 1535(2): p. 145-52.
73. Vaishnav, R.A., et al., Lipid peroxidation-derived reactive aldehydes directly and differentially impair spinal cord and brain mitochondrial function. *J Neurotrauma*, 2010. 27(7): p. 1311-20.
74. Fiore, C., et al., The mitochondrial ADP/ATP carrier: structural, physiological and pathological aspects. *Biochimie*, 1998. 80(2): p. 137-50.
75. Klingenberg, M. and D.R. Nelson, Structure-function relationships of the ADP/ATP carrier. *Biochim Biophys Acta*, 1994. 1187(2): p. 241-4.
76. Dutta, R. and B.D. Trapp, Pathogenesis of axonal and neuronal damage in multiple sclerosis. *Neurology*, 2007. 68(22 Suppl 3): p. S22-31; discussion S43-54.

77. Kandel, E.R., J.H. Schwartz, and T.M. Jessell, Principles of neural science. 4th ed. 2000, New York: McGraw-Hill, Health Professions Division. xli, 1414 p.
78. Shi, R., The dynamics of axolemmal disruption in guinea pig spinal cord following compression. *J Neurocytol*, 2004. 33(2): p. 203-11.
79. Shi, R., et al., Control of membrane sealing in injured mammalian spinal cord axons. *J Neurophysiol*, 2000. 84(4): p. 1763-9.
80. Shi, R. and J.D. Pryor, Pathological changes of isolated spinal cord axons in response to mechanical stretch. *Neuroscience*, 2002. 110(4): p. 765-77.
81. Leung, G., et al., Potassium channel blocker, 4-aminopyridine-3-methanol, restores axonal conduction in spinal cord of an animal model of multiple sclerosis. *Exp Neurol*, 2011. 227(1): p. 232-5.
82. Luo, J., R. Borgens, and R. Shi, Polyethylene glycol immediately repairs neuronal membranes and inhibits free radical production after acute spinal cord injury. *J Neurochem*, 2002. 83(2): p. 471-80.
83. Luo, J., R. Borgens, and R. Shi, Polyethylene glycol improves function and reduces oxidative stress in synaptosomal preparations following spinal cord injury. *J Neurotrauma*, 2004. 21(8): p. 994-1007.
84. Shi, R. and R.B. Borgens, Acute repair of crushed guinea pig spinal cord by polyethylene glycol. *J Neurophysiol*, 1999. 81(5): p. 2406-14.
85. Borgens, R.B. and R. Shi, Immediate recovery from spinal cord injury through molecular repair of nerve membranes with polyethylene glycol. *FASEB J*, 2000. 14(1): p. 27-35.
86. Shi, R. and R.B. Borgens, Anatomical repair of nerve membranes in crushed mammalian spinal cord with polyethylene glycol. *J Neurocytol*, 2000. 29(9): p. 633-43.
87. Nehrt, A., et al., Polyethylene glycol enhances axolemmal resealing following transection in cultured cells and in ex vivo spinal cord. *J Neurotrauma*, 2010. 27(1): p. 151-61.
88. Bjartmar, C., et al., Neurological disability correlates with spinal cord axonal loss and reduced N-acetyl aspartate in chronic multiple sclerosis patients. *Ann Neurol*, 2000. 48(6): p. 893-901.
89. Schlaepfer, W.W. and R.P. Bunge, Effects of calcium ion concentration on the degeneration of amputated axons in tissue culture. *J Cell Biol*, 1973. 59(2 Pt 1): p. 456-70.

90. Xie, X.Y. and J.N. Barrett, Membrane resealing in cultured rat septal neurons after neurite transection: evidence for enhancement by Ca(2+)-triggered protease activity and cytoskeletal disassembly. *J Neurosci*, 1991. 11(10): p. 3257-67.
91. Chen, H., et al., Polyethylene glycol protects injured neuronal mitochondria. *Pathobiology*, 2009. 76(3): p. 117-28.
92. Luo, J. and R. Shi, Polyethylene glycol inhibits apoptotic cell death following traumatic spinal cord injury. *Brain Res*, 2007. 1155: p. 10-6.
93. Sinkuvenc, D.S., [Hygienic assessment of acrolein as an air pollutant]. *Gig Sanit*, 1970. 35(3): p. 6-10.
94. Cahill, T.M., et al., Development and application of a sensitive method to determine concentrations of acrolein and other carbonyls in ambient air. *Res Rep Health Eff Inst*, 2010(149): p. 3-46.
95. Luo, J., K. Uchida, and R. Shi, Accumulation of acrolein-protein adducts after traumatic spinal cord injury. *Neurochem Res*, 2005. 30(3): p. 291-5.
96. Osorio, V.M. and Z. de Lourdes Cardeal, Determination of acrolein in french fries by solid-phase microextraction gas chromatography and mass spectrometry. *J Chromatogr A*, 2011. 1218(21): p. 3332-6.
97. Uchida, K., et al., Protein-bound acrolein: potential markers for oxidative stress. *Proc Natl Acad Sci U S A*, 1998. 95(9): p. 4882-7.
98. Hamann, K. and R. Shi, Acrolein scavenging: a potential novel mechanism of attenuating oxidative stress following spinal cord injury. *J Neurochem*, 2009. 111(6): p. 1348-56.
99. Yan, W., et al., Development and validation of a direct LC-MS-MS method to determine the acrolein metabolite 3-HPMA in urine. *J Chromatogr Sci*, 2010. 48(3): p. 194-9.
100. Zheng, L., et al., Determination of urine 3-HPMA, a stable acrolein metabolite in a rat model of spinal cord injury. *J Neurotrauma*, 2013. 30(15): p. 1334-41.
101. Abraham, K., et al., Toxicology and risk assessment of acrolein in food. *Mol Nutr Food Res*, 2011. 55(9): p. 1277-90.
102. Wang, H., et al., Direct analysis of biological tissue by paper spray mass spectrometry. *Anal Chem*, 2011. 83(4): p. 1197-201.

103. LoPachin, R.M., D.S. Barber, and T. Gavin, Molecular mechanisms of the conjugated alpha,beta-unsaturated carbonyl derivatives: relevance to neurotoxicity and neurodegenerative diseases. *Toxicol Sci*, 2008. 104(2): p. 235-49.
104. Carmella, S.G., et al., Quantitation of acrolein-derived (3-hydroxypropyl)mercapturic acid in human urine by liquid chromatography-atmospheric pressure chemical ionization tandem mass spectrometry: effects of cigarette smoking. *Chem Res Toxicol*, 2007. 20(7): p. 986-90.
105. Carmines, E.L. and C.L. Gaworski, Toxicological evaluation of glycerin as a cigarette ingredient. *Food Chem Toxicol*, 2005. 43(10): p. 1521-39.
106. Ascherio, A. and K.L. Munger, Environmental risk factors for multiple sclerosis. Part II: Noninfectious factors. *Ann Neurol*, 2007. 61(6): p. 504-13.
107. Ebers, G.C., Environmental factors and multiple sclerosis. *Lancet Neurol*, 2008. 7(3): p. 268-77.
108. Hammond, S.R., D.R. English, and J.G. McLeod, The age-range of risk of developing multiple sclerosis: evidence from a migrant population in Australia. *Brain*, 2000. 123 (Pt 5): p. 968-74.
109. Handel, A.E., et al., Environmental factors and their timing in adult-onset multiple sclerosis. *Nat Rev Neurol*, 2010. 6(3): p. 156-66.
110. Hedstrom, A.K., et al., Tobacco smoking, but not Swedish snuff use, increases the risk of multiple sclerosis. *Neurology*, 2009. 73(9): p. 696-701.
111. Friend, K.B., et al., Smoking rates and smoking cessation among individuals with multiple sclerosis. *Disabil Rehabil*, 2006. 28(18): p. 1135-41.
112. Tully, M., et al., Acute systemic accumulation of acrolein in mice by inhalation at a concentration similar to that in cigarette smoke. *Neurosci Bull*, 2014. 30(6): p. 1017-24.
113. Schettgen, T., A. Musiol, and T. Kraus, Simultaneous determination of mercapturic acids derived from ethylene oxide (HEMA), propylene oxide (2-HPMA), acrolein (3-HPMA), acrylamide (AAMA) and N,N-dimethylformamide (AMCC) in human urine using liquid chromatography/tandem mass spectrometry. *Rapid Commun Mass Spectrom*, 2008. 22(17): p. 2629-38.
114. Anders, M.W., J.L. Robotham, and S.S. Sheu, Mitochondria: new drug targets for oxidative stress-induced diseases. *Expert Opin Drug Metab Toxicol*, 2006. 2(1): p. 71-9.

115. Dong, J.Z. and S.C. Moldoveanu, Gas chromatography-mass spectrometry of carbonyl compounds in cigarette mainstream smoke after derivatization with 2,4-dinitrophenylhydrazine. *J Chromatogr A*, 2004. 1027(1-2): p. 25-35.
116. Faroon, O., et al., Acrolein environmental levels and potential for human exposure. *Toxicol Ind Health*, 2008. 24(8): p. 543-64.
117. Faroon, O., et al., Acrolein health effects. *Toxicol Ind Health*, 2008. 24(7): p. 447-90.
118. Struve, M.F., et al., Nasal uptake of inhaled acrolein in rats. *Inhal Toxicol*, 2008. 20(3): p. 217-25.
119. Turner, C.R., et al., Acrolein increases airway sensitivity to substance P and decreases NEP activity in guinea pigs. *J Appl Physiol* (1985), 1993. 74(4): p. 1830-9.
120. Turner, C.R., et al., Protective role for neuropeptides in acute pulmonary response to acrolein in guinea pigs. *J Appl Physiol* (1985), 1993. 75(6): p. 2456-65.
121. Wheat, L.A., et al., Acrolein inhalation prevents vascular endothelial growth factor-induced mobilization of Flk-1+/Sca-1+ cells in mice. *Arterioscler Thromb Vasc Biol*, 2011. 31(7): p. 1598-606.

VITA

VITA

Melissa Tully was born in Indianapolis, IN and moved to East Patchogue, NY when she was 6 years old. Upon graduating from high school in 2005, she attended Stony Brook University where she earned a Bachelor's degree in Biomedical Engineering in 2009. Melissa was then accepted to the Medical Scientist Training Program at Indiana University School of Medicine and completed two years of medical school prior to pursuing a Ph.D. in biomedical engineering at Purdue University. She joined the Laboratory of Translational Neuroscience under the advisement of Dr. Riyi Shi and has spent the last four years in his laboratory investigating the role of both endogenously and exogenously produced acrolein in clinical cases and animal models of MS. Upon the completion of her Ph.D., Melissa will return to IUSM to complete her final two years of medical training and earn an M.D

PUBLICATIONS

PUBLICATIONS

- Du C, **Tully M**, Volkow ND, Schiffer WK, Yu M, Luo Z, Koretsky AP, Benveniste H. Differential effects of anesthetics on cocaine's pharmacokinetic and pharmacodynamic effects in brain. (2009) *Eur J Neurosci*, 30(8): 1565-57.
- Luo Z, Yuan Z, **Tully M**, Pan Y, Du C. Quantification of cocaine-induced cortical blood flow changes using laser speckle contrast imaging and Doppler optical coherence tomography. (2009) *Appl Opt*, 48(10): D247-55.
- Leung G, Sun W, Zheng L, Brookes S, **Tully M**, Shi R. Anti-acrolein treatment improves behavioral outcome and alleviates myelin damage in experimental autoimmune encephalomyelitis mouse. (2011) *Neuroscience*, (26)173:150-5.
- Zheng L, Park J, Walls M, **Tully M**, Jannasch A, Cooper B, Shi R. Determination of urine 3-HPMA, a stable acrolein metabolite in a rat model of spinal cord injury. (2013) *J Neurotrauma*, 30(15): 1334-41.
- Tully M**, Shi R. New insights in the pathogenesis of multiple sclerosis—role of acrolein in neuronal and myelin damage. (2013) *Int J Mol Sci*, 14(10): 20037-47.
- Tully M**, Zheng L, Shi R. Acrolein detection: Potential theranostic utility in multiple sclerosis and spinal cord injury. (2014) *Expert Rev Neurother*, 14(6): 679-85.
- Tully M**, Zheng L, Acosta G, Tian R, Shi R. Acute systemic accumulation of acrolein in mice by inhalation at a concentration similar to that in cigarette smoke. (2014) *Neurosci Bull*, 30(6): 1017-24.
- Shi R, Page J, **Tully M**. Molecular mechanisms of acrolein-mediated myelin destruction in CNS trauma and disease. (2015) *Free Radical Res*, *In press*.